L-295

NATIONAL ADVISORY COMMITTEE FOR AERONAUTICS

WARTIME REPORT

ORIGINALLY ISSUED
January 1943 as
Advance Restricted Report

WIND-TUNNEL TESTS OF A TWIN-ENGINE MODEL TO DETERMINE THE EFFECT OF DIRECTION OF PROPELLER ROTATION ON THE STATIC-STABILITY CHARACTERISTICS

By Francis M. Rogallo and Robert S. Swanson

Langley Memorial Aeronautical Laboratory
Langley Field, Va.

NACA

WASHINGTON

NATIONAL ADVISORY COMMITTEE FOR AERONAUTICS

ADVANCE RESTRICTED REPORT

WIND-TUNNEL TESTS OF A TWIN-ENGINE MODEL TO DETERMINE THE EFFECT OF DIRECTION OF PROPELLER ROTATION ON THE STATIC-STABILITY CHARACTERISTICS

By Francis M. Rogallo and Robert S. Swanson

SUMMARY

Tests were made in the LMAL 7- by 10-foot tunnel to determine the effect of direction of propeller rotation on the static longitudinal- and lateral-stability characteristics of the 1/10-scale model of the North American B-28 airplane.

The results of the present investigation indicate that the mode of propeller operation has a considerable effect upon lateral and longitudinal stability and may have an effect upon propulsive efficiency. The best mode of rotation from consideration of stability is dependent upon the flight condition and also upon the configuration of the airplane.

INTRODUCTION

Tests were made in the LMAL 7- by 10-foot tunnel to determine the effect of the direction of propeller rotation on the effective thrust coefficients and the static longitudinal- and lateral-stability characteristics of the 1/10-scale model of the North American XB-28 airplane. Most of the tests were repeated with each of three modes of propeller rotation: tips of both propellers coming up in the center (designated $P_{1L}P_{2R}$), tips of both propellers going down in the center ($P_{1R}P_{2L}$), and right-hand rotation of both propellers ($P_{1R}P_{2R}$). Power-on static-stability tests were made of the wing alone, of the wing and fuselage, and of the wing, fuselage, and tail with the model in the high-speed condition and in the landing condition. With the model in the landing condition, high-lift flaps were added below and ahead of the ailerons to simulate a full-span duplex-flap arrangement. (See reference 1.) A few

power-off tests were made of the ailerons in combination with this flap arrangement.

Four additional tests were made to indicate the effect of mode of propeller rotation upon effective thrust coefficients. A brief discussion of the test results is included.

It is desired to acknowledge the courtesy of North American Aviation, Inc., in making their model available for this investigation after the completion of the original program for the model.

MODEL

The 1/10-scale model of the North American XB-28 airplane was furnished by North American Aviation, Inc. and no attempt was made to check its dimensions. The propeller modes and the model designations used in this report are those of North American Aviation, Inc. A three-view drawing of the complete airplane without the duplex flaps indicated is shown in figure 1. In figure 2(a) a three-quarter front view of the complete model with duplex flaps deflected, landing gear extended, and propellers on is shown mounted in the tunnel. Figure 2(b) is a three-quarter rear view of the model in the same condition. In figure 3(a) is shown a three-quarter front view of the wing with duplex flaps deflected, split flap deflected over the center section normally covered by fuselage (only a few wing-alone landing-condition tests were run with split flaps in the center section), landing gear extended, and propellers on as mounted in the tunnel. In figure 3(b) is shown the same model configuration but from a three-quarter rear view. A typical section of the outboard flap of the duplex flap arrangement is shown in figure 4.

The fuselage fillets were made of fillet wax. The angle of attack of the reference line was determined by means of leveling bar furnished with the model. The flap and control-surface deflections were set by means of templets. The propeller-blade angles at the 75-percent-radius station were set by means of a protractor. The turrets and the periscopes were not installed.

OPERATING PROCEDURE

No equipment was readily available to measure the torque or power output of the model motors. For this reason the only power parameters determined were the propeller-blade

angle, the effective thrust coefficient, and the advance-diameter ratio.

The test procedure adopted (see reference 2) was to make propeller-calibration tests (fig. 5) at the propeller-blade angles and the tunnel speed (in order to eliminate Reynolds number effects) to be used for the tests. The calibration was made for only one mode of rotation but was used for all modes of rotation. For each test the propeller speed was adjusted in such a way that for each lift coefficient the effective thrust coefficient, as determined from figure 5, matched the effective thrust coefficients of the airplane. The airplane power conditions are given in figure 6. The yaw tests were made at a constant value of propeller speed corresponding to the proper value of effective thrust coefficient for zero angle of yaw.

TESTS AND RESULTS

Test conditions.- The tests were made in the LMAL 7- by 10-foot tunnel. (See reference 3.) All the tests with flaps neutral were run at a dynamic pressure of 16.37 pounds per square foot, which corresponds to a velocity of about 80 miles per hour under standard sea-level conditions and to a test Reynolds number of about 730,000, based on the mean aerodynamic chord of 12.009 inches. The effective Reynolds number R_e was about 1,170,000, based on a turbulence factor of 1.6 for the 7- by 10-foot tunnel. The tests with flaps deflected were run at a dynamic pressure of 4.09 pounds per square foot, which corresponds to a velocity of about 40 miles per hour under standard sea-level conditions, a test Reynolds number of about 365,000, and an effective Reynolds number of about 585,000.

Coefficients.- The results of the tests are given in the form of standard NACA coefficients of forces and moments based on model wing area, wing span, and mean aerodynamic chord. All moments are given about the center-of-gravity location on the fuselage reference line and at 26 percent of the mean aerodynamic chord. The data are referred to the stability axes, a system in which the X axis is the intersection of the plane of symmetry of the airplane with a plane perpendicular to the plane of symmetry and parallel to the relative wind direction, the Y axis is perpendicular to the plane of symmetry, and the Z axis is in the plane of symmetry and perpendicular to the X axis. In

other words, the stability axes are the regular NACA wind axes rotated in yaw with the model. The coefficients are defined as follows:

C_D drag coefficient, propellers removed (X/qS)

C_{D_R} resultant drag coefficient (X/qS)

C_Y lateral-force coefficient (Y/qS)

C_L lift coefficient (Z/qS)

C_l rolling-moment coefficient about center of gravity (l/qSb)

C_m pitching-moment coefficient about center of gravity (m/qSc)

C_n yawing-moment coefficient about center of gravity (n/qSb)

C_{Y_ψ} static lateral-force derivative $\left(\frac{\partial C_Y}{\partial \psi}\right)$

C_{l_ψ} static rolling-moment derivative $\left(\frac{\partial C_l}{\partial \psi}\right)$

C_{n_ψ} static yawing-moment derivative $\left(\frac{\partial C_n}{\partial \psi}\right)$

T_c' effective model thrust coefficient (T_e'/qS)

T_c effective propeller thrust coefficient $\frac{T_e}{\rho V^2 D^2} = 0.876 \times T_c'$

where

X force along X axis, positive when directed backward

Y force along Y axis, positive when directed to right

Z force along Z axis, positive when directed upward

l rolling moment about X axis, positive when it tends to depress right wing

m pitching moment about Y axis, positive when it tends to depress tail

n yawing moment about the Z axis, positive when it tends to retard right wing

q dynamic pressure $\left(\frac{1}{2}\rho V^2\right)$ (16.37 or 4.09 lb/sq ft)

S wing area (6.759 sq ft)

c mean aerodynamic chord (1.001 ft)

b wing span (7.261 ft)

V/nD advance-diameter ratio

T_e effective thrust per engine, pounds

T_e' total effective thrust, pounds

ρ mass density of air, slugs per cubic foot

V airspeed, feet per second

D propeller diameter (1.388 ft)

n propeller speed, revolutions per second

N propeller speed, revolutions per minute

and

α angle of attack of fuselage reference line, degrees

α_u uncorrected angle of attack of fuselage reference line, degrees

ψ angle of yaw, positive when nose of model moves to right, degrees

i_t angle of stabilizer setting with respect to fuselage reference line, positive when trailing edge moves down, set at 1.5°, degrees

δ_a aileron deflection with respect to wing chord, positive when trailing edge of aileron moves down, degrees

δ_f flap deflection, positive when trailing edge of flap moves down, degrees

δ_e elevator deflection, positive when trailing edge of elevator moves down, degrees

δ_r rudder deflection, positive when trailing edge of rudder moves to left, degrees

β angle of propeller-blade setting at the 75-percent-radius station

Subscripts:

R right

1 inboard portion of duplex flap

2 outboard portion of duplex flap

Corrections.- The lift, drag, and pitching-moment coefficients, except for the wing alone, have been approximately corrected for tares caused by the model support. These tares for the complete model, with propellers off and at zero yaw only, are given in table I. They were obtained from tests of a similar model with a dummy support. No tare corrections were made for the wing alone.

The angle of attack, the drag coefficients, and the pitching-moment coefficients have been corrected for the effects of the tunnel walls. The jet-boundary corrections applied were computed as follows:

Induced-drag correction,

$$\Delta C_{D_i} = \delta \frac{S}{C} C_L^{\,2} \qquad (1)$$

Induced angle-of attack correction,

$$\Delta \alpha_i = \delta \frac{S}{C} C_L \, (57.3) \qquad (2)$$

Pitching-moment-coefficient correction,

$$\Delta C_m = \delta_a \frac{S}{C} \frac{dC_m}{di_t} C_L \, (57.3) \sqrt{q_o/q_s} \qquad (3)$$

All corrections are added to tunnel data. In equations (1), (2), and (3):

$\delta = 0.114$

$\delta_a = 0.080$

C tunnel cross-sectional area (69.59 sq ft)

$\frac{dC_m}{di_t}$ change in pitching-moment coefficient per degree change in stabilizer setting as determined from previous tests of model with flaps neutral and deflected and with power on and power off

q_o free-stream dynamic pressure

q_s average dynamic pressure across tail span

Substitution of the various factors in the equation gives the following simple, approximate formula for flaps either neutral or deflected, power on or power off:

$$\Delta C_m = 0.015\ C_L$$

No jet-boundary corrections were made to the rolling-moment or yawing-moment coefficients. The corrections may be applied by use of the following approximate formulas, which were derived for the unyawed model but which may be used to correct the lateral and directional stability criterions determined at small angles of yaw:

$$\Delta C_{l_{y_c}} = 0.974\ \Delta C_{l_{y_u}} \tag{4}$$

$$\Delta C_{n_{y_c}} = \Delta C_{n_{y_u}} - 0.016\ \Delta C_{l_{y_u}}\ C_L + 0.074\ \Delta C_{l_{y_u}}{}^2 \tag{5}$$

where the subscripts may be defined as follows:

y increments due to yaw (dihedral effect)

c corrected values

u uncorrected values, which are given, without subscripts, in the figures of test results

It should be emphasized that the increments of rolling moments and lift coefficients used in equations (4) and (5) are due to the wing and flaps alone and do not include the effects of power, model asymmetry, the tail surfaces, or the fuselage in producing lift or rolling moment.

For convenience in locating the results, a résumé of the tests and of figures in which the results are presented is given in table II. Also, the abbreviations used to designate the various model conditions are given.

DISCUSSION

Power-on static-stability tests were made of the wing alone, the wing and fuselage, and the wing, the fuselage, and the tail surfaces for three modes of propeller rotation and two representative model conditions. The tests are, of course, not complete enough to determine interference effects, but they do provide some insight into the contribution of the various components of the model to its stability characteristics for the conditions tested. The pitch tests were made at $\pm 5^{\circ}$ yaw and were used not only to obtain a measure of the lateral-stability derivatives but also as a measure of the longitudinal-stability characteristics of the model. This method of obtaining longitudinal-stability characteristics is considered to give a reasonably good approximation, and its accuracy may be estimated from the data presented for the yaw tests, which show the difference between the pitching moment at 0° yaw and $\pm 5^{\circ}$ yaw. In any case the lift, drag, and pitching-moment data are presented for both the $\pm 5^{\circ}$ yaw runs in pitch.

The maximum lift coefficient of the model with full-span duplex flaps was about the same as obtained in unpublished tests previously made on the same model with partial-span flaps because of the manner in which the wing stalled. The stall might occur differently at full-scale Reynolds number. Below the stall the addition of the flaps at the wing tips increased the lift coefficient by about the expected amount and, relative to their effect upon the stability of the model, the duplex flaps were thought to be representative of practical arrangements of full-span flaps.

Some of the wing-alone tests, with the wing in landing conditions, were repeated with split flaps added to the center section normally occupied by the fuselage (fig. 3).

The static-stability data are presented in figures 7 to 18, which show the effect of mode of propeller rotation on the various characteristics in yaw and in pitch for each model and power condition tested. Tests with the propeller removed are presented for the landing condition for comparison. It was not considered necessary to discuss the

figures individually; only general trends are pointed out. The resumé of the tests, previously given, and the titles on the figures are self-explanatory.

Longitudinal stability.- The curves showing the variation of pitching moment with angle of attack indicate that mode of rotation has some effect on the magnitude of the pitching-moment (trim) but has little effect on the static longitudinal stability for the wing alone or for the wing plus fuselage. The fuselage is destabilizing. The wing alone with flaps neutral is unstable; the wing alone with flaps deflected is slightly stable; and the wing alone with fuselage and flaps is just about neutrally stable. The tail surfaces are stabilizing for all modes of rotation on the clean model and for rotation mode $P_{1R}P_{2L}$ on the model with flaps deflected. The tail surfaces do not materially change the stability for the model with flaps deflected and rotation mode $P_{1R}P_{2R}$ but decrease the stability slightly for rotation mode $P_{1L}P_{2R}$. The complete model with flaps neutral has the greatest stability with rotation mode $P_{1L}P_{2R}$, is slightly less stable with mode $P_{1R}P_{2R}$, and is least stable (even unstable over high angle-of-attack range) with rotation mode $P_{1R}P_{2L}$ (fig. 17). The complete model with duplex flaps deflected, however, has the greatest stability with mode $P_{1R}P_{2L}$, is slightly less stable with mode $P_{1R}P_{2R}$, and has the least stability with mode $P_{1L}P_{2R}$. The difference in stability and trim of modes $P_{1R}P_{2R}$ and $P_{1L}P_{2R}$ with the duplex flaps is about the same as with the partial-span flaps, as shown by unpublished data. It is probable that these two modes of rotation would give about the same stability if the tail setting was adjusted to give the same trim.

The contrasting effects of mode of propeller operation upon the stability for the conditions with flaps neutral and with flaps deflected are rather difficult to explain. Only the main arguments as they apply to this model are indicated although several different effects must be considered in the general case. For the condition with flaps neutral the sheared and slightly distorted slipstream passes over the tail and the effects of slipstream rotation are as would be expected. For the condition with flaps deflected, however, the increased downwash displaces the slipstream further downward and the slipstream shearing, the rotation damping, and the distortions are greatly increased. The direct effect of rotation is almost entirely eliminated at the normal tail location, since the slipstream passes below the tail,

and therefore the main component of rotation is along the tail span (sidewash) rather than normal to the tail span (downwash). The indirect effect of rotation is thus more important for the condition with flaps deflected than for the condition with flaps neutral. This indirect effect is simply that a different portion of the sheared and distorted slipstream field is passed near the normal tail location for the different modes of rotation. The portion of the downwash field near the normal tail is more destabilizing for the propellers rotating up in the center for this model. Air-flow surveys behind similar twin-engine models made at the Laboratory also showed this difference in the effects of mode of propeller rotation on the downwash.

Longitudinal trim changes in yaw.- The variation of pitching moment with angle of yaw is apparently a complex function of the mode of rotation and the model condition. The curves of pitching-moment coefficient against angle of yaw were reasonably symmetrical about the zero yaw axis for all model conditions for the symmetrical modes of rotation ($P_{1L}P_{2R}$ and $P_{1R}P_{2L}$). For the unsymmetrical mode ($P_{1R}P_{2R}$) there was a marked increase in the stalling moment over the positive yaw range and a marked decrease in the stalling moment over the negative yaw range for the wing-alone cases (figs. 7 and 8). The addition of the fuselage reduced the difference between the unsymmetrical mode and the symmetrical modes. The further addition of the tail (complete model) resulted in a very unsymmetrical pitching-moment angle-of-yaw curve for the unsymmetrical mode of rotation. The magnitude of the increment of pitching moment due to yaw is, in general, large for the complete-model condition.

Directional stability.- Power increases the directional instability of the wing with flaps. The fuselage increases the instability. The tail surfaces make the model stable. Mode of rotation does not appear to have a great deal of effect upon the stability for the condition with flaps neutral but has some effect for the condition with flaps deflected. It appears from figure 18 that for an α greater than 5°, $P_{1R}P_{2L}$ is the most stable mode, $P_{1R}P_{2R}$ next, and $P_{1L}P_{2R}$ the least stable; for α less than 5° the order is reversed.

Directional trim.- The mode of propeller rotation has a large effect on directional trim and on the general shape of the yawing-moment curves for the condition with flaps

deflected. The smallest changes in trim due to propeller operation are associated with the symmetrical rotation modes.

Rolling stability.- The model with flaps neutral is stable in roll with all rotation modes. Mode $P_{1R}P_{2L}$ is, in general, the most stable, $P_{1R}P_{2R}$ next, and $P_{1L}P_{2R}$ the least stable. With flaps deflected the model is stable only in the low-lift range with power. The tail surfaces are stabilizing. In the high-lift range the least loss in stability due to propeller operation is obtained by use of mode $P_{1R}P_{2L}$, the other modes being approximately equal over this range. The greatest stability, however, over the low-lift range resulted from the use of mode $P_{1L}P_{2R}$.

Lift and effective thrust.- The mode of rotation $P_{1L}P_{2R}$ (with the tips of both propellers coming up in the center) gave the highest lift and greatest effective thrust; the mode of rotation $P_{1R}P_{2R}$ (with both right-hand propellers) gave a medium value of lift and effective thrust; and the mode of rotation $P_{1R}P_{2L}$ (with the propeller tips going down in center) gave the lowest lift and effective thrust for a given angle of attack for the model. The special effective-thrust tests (figs. 19 and 20) also showed this effect. Although the torque was not directly determined, there was no measurable difference in the minimum current input to the motors (an indication of the torque for these motors) due to mode of rotation. The effective thrust-coefficient data of figure 19 were computed directly from the measured power-on and power-off drags of the model at the given tunnel angles of attack; that is, the data are uncorrected for the increased induced drag due to the increased lift resulting from the action of the slipstream. The increase in effective thrust for rotation mode $P_{1L}P_{2R}$ over that for $P_{1R}P_{2L}$ appears to be due to better wing-nacelle interference for the rotation mode with propeller tips coming up on the inboard side of the nacelle; that is, the slipstream twist accompanying this mode of rotation improves the pressure recovery over the nacelles.

This interpretation is supported by subsequent tests of a model of another twin-engine airplane, in which the most efficient mode of rotation was found to be with the tips of both propellers going down in the center. The difference of model configuration is thought to account for the difference of interference effects.

Because of the low scale of the present tests and the large variation of interference phenomena that may accompany changes of scale, it is recommended that the effect of mode of propeller rotation on propulsive efficiency be determined at higher Reynolds numbers. The lift data of figure 20 include all components of lift acting on the wing-propeller unit. The thrust component in the negative lift direction is apparently the greatest component of lift for the runs at $\alpha_u = -4.8^\circ$.

Power-off aileron tests.- The effects of aileron deflection on the aerodynamic characteristics of the model in the landing condition at zero yaw, power off, are shown in figure 21. The aileron rolling-moment effectiveness is not linear and falls off rapidly with positive deflections greater than about 10°, possibly because of the low scale of the tests. The amount of rolling moment due to an aileron deflection of -20° varies markedly with model attitude.

More recent unpublished tests of ailerons with duplex flaps on a large semispan wing showed that the ailerons probably would have been more powerful provided, the balanced split flaps had been located farther below the wing (larger gap) and farther back. The change in lift characteristics due to moving the flap to this new position appeared to be negligible.

CONCLUDING REMARKS

The results of the present investigation indicate that the mode of propeller operation has a considerable effect upon lateral and longitudinal stability and may have an effect upon propulsive efficiency. The best mode of rotation from considerations of stability is dependent upon the flight condition and also upon the configuration of the airplane. Oppositely rotating propellers with the tips coming up in the center appeared to give the highest propulsive efficiency for the wing-nacelle arrangement used in the tests. Because this effect was attributed to interference, it should be carefully checked at higher Reynolds numbers. Only a brief analysis has thus far been made of the results of the present investigation.

Langley Memorial Aeronautical Laboratory,
National Advisory Committee for Aeronautics,
Langley Field, Va.

REFERENCES

1. Harris, Thomas A., and Purser, Paul E.: Wind-Tunnel Investigation of Plain Ailerons for a Wing with a Full-Span Flap Consisting of an Inboard Fowler and an Outboard Retractable Split Flap. NACA A.C.R., March 1941.

2. Recant, Isidore G., and Swanson, Robert S.: Determination of the Stability and Control Characteristics of Airplanes from Tests of Powered Models. NACA A.R.R., July 1942.

3. Wenzinger, Carl J., and Harris, Thomas A.: Wind-Tunnel Investigation of an N.A.C.A. 23012 Airfoil with Various Arrangements of Slotted Flaps. Rep. No. 664, NACA, 1939.

TABLE I

SUPPORT STRUT TARES USED IN COMPUTING THE COEFFICIENTS

[Tares were determined for a model similar to the XB-28 model]

α_u (deg)	ΔC_L	ΔC_D	ΔC_m
-10	-0.004	0.0062	-0.003
-9	-.002	.0062	-.003
-8	-.001	.0056	-.003
-7	.001	.0053	-.003
-6	.002	.0049	-.003
-5	.002	.0046	-.003
-4	.001	.0043	-.003
-3	-.001	.0039	-.002
-2	-.002	.0037	-.002
-1	-.004	.0033	-.002
0	-.006	.0031	-.002
.5	-.007	.0029	-.002
1	-.008	.0028	-.002
2	-.009	.0025	-.002
3	-.007	.0022	-.002
4	-.005	.0020	-.002
5	-.003	.0017	-.002
6	-.002	.0015	-.002
7	-.001	.0012	-.001
8	-.001	.0010	-.001
10.6	0	0	0

RÉSUMÉ OF TESTS AND FIGURES

Test	Model description								ψ (deg) (b)	α_u (deg) (b)	Power condition	q (lb/sq ft)	Figure
	Configuration	Condition	Propeller rotation mode (a)	β' (deg)	δ_a (deg)	δ_e (deg)	δ_r (deg)	i_t (deg)					
110	Wing+fuselage	High-speed	$P_{1R}P_{2L}$	40.5	0				5		[c]Rated power	16.37	13
111	---- do -----	--- do ---	- do -	40.5	0					7.8	-do--	16.37	11
112	---- do -----	--- do ---	- do -	40.5	0				-5		-do--	16.37	13
113	---- do -----	--- do ---	$P_{1L}P_{2R}$	40.5	0				-5		-do--	16.37	13
114	---- do -----	--- do ---	- do -	40.5	0					7.8	-do--	16.37	11
115	---- do -----	--- do ---	- do -	40.5	0				5		-do--	16.37	13
116	---- do -----	--- do ---	$P_{1R}P_{2R}$	40.5	0				5		-do--	16.37	13
117	---- do -----	--- do ---	- do -	40.5	0					7.8	-do--	16.37	11
118	---- do -----	--- do ---	- do -	40.5	0				-5		-do--	16.37	13
119	Complete model	--- do ---	- do -	40.5	0	0	0	1.5	-4.9		-do--	16.37	17
120	---- do -----	--- do ---	- do -	40.5	0	0	0	1.5		7.8	-do--	16.37	15
121	---- do -----	--- do ---	- do -	40.5	0	0	0	1.5	4.8		-do--	16.37	17
122	---- do -----	--- do ---	$P_{1L}P_{2R}$	40.5	0	0	0	1.5	4.8		-do--	16.37	17
123	---- do -----	--- do ---	- do -	40.5	0	0	0	1.5		7.8	-do--	16.37	15
124	---- do -----	--- do ---	- do -	40.5	0	0	0	1.5	-4.9		-do--	16.37	17
125	---- do -----	--- do ---	$P_{1R}P_{2L}$	40.5	0	0	0	1.5	-4.9		-do--	16.37	17
126	---- do -----	--- do ---	- do -	40.5	0	0	0	1.5		7.8	-do--	16.37	15
127	---- do -----	--- do ---	- do -	40.5	0	0	0	1.5	4.8		-do--	16.37	17
128	Wing alone	--- do ---	- do -	40.5	0				5		-do--	16.37	9
129	---- do -----	--- do ---	- do -	40.5	0					7.8	-do--	16.37	7
130	---- do -----	--- do ---	- do -	40.5	0				-5		-do--	16.37	9
131	---- do -----	--- do ---	$P_{1L}P_{2R}$	40.5	0				-5		-do--	16.37	9
132	---- do -----	--- do ---	- do -	40.5	0					7.8	-do--	16.37	7
133	---- do -----	--- do ---	- do -	40.5	0				5		-do--	16.37	9
134	---- do -----	--- do ---	$P_{1R}P_{2R}$	40.5	0				5		-do--	16.37	9
135	---- do -----	--- do ---	- do -	40.5	0					7.8	-do--	16.37	7
136	---- do -----	--- do ---	- do -	40.5	0				-5		-do--	16.37	9
137	Complete model	Landing			[d]-30	0	0	1.5	0		No propellers	4.09	21
138	---- do -----	--- do ---			[d]-20	0	0	1.5	0		-do--	4.09	21
139	---- do -----	--- do ---			[d]-10	0	0	1.5	0		-do--	4.09	21
140	---- do -----	--- do ---			[d]0	0	0	1.5	0		-do--	4.09	21
141	---- do -----	--- do ---			[d]10	0	0	1.5	0		-do--	4.09	21
142	---- do -----	--- do ---			[d]20	0	0	1.5	0		-do--	4.09	21
143	---- do -----	--- do ---	$P_{1R}P_{2L}$	27.1	0	0	0	1.5	5		[e]Take-off power	4.09	18
144	---- do -----	--- do ---	- do -	27.1	0	0	0	1.5		6.8	-do--	4.09	16
145	---- do -----	--- do ---	- do -	27.1	0	0	0	1.5	-5		-do--	4.09	18
146	---- do -----	--- do ---	$P_{1L}P_{2R}$	27.1	0	0	0	1.5	-5		-do--	4.09	18
147	---- do -----	--- do ---	- do -	27.1	0	0	0	1.5		6.8	-do--	4.09	16
148	---- do -----	--- do ---	- do -	27.1	0	0	0	1.5	5		-do--	4.09	18

[a]Definition of symbols:

P_{1R} left-hand motor, right-hand propeller

P_{2R} right-hand motor, right-hand propeller

P_{1L} left-hand motor, left-hand propeller

P_{2L} right-hand motor, left-hand propeller

[b]Range of values indicated when numerical values are omitted.

[c]1625 hp at 25,000 ft.

[d]Values of δ_{a_R}.

[e]2000 hp at sea level.

L-295

RÉSUMÉ OF TESTS AND FIGURES - Continued

Test	Model description								ψ (deg) (b)	α_u (deg) (b)	Power condition	q (lb/sq ft)	Figure
	Configuration	Condition	Propeller rotation mode (a)	β (deg)	δ_a (deg)	δ_e (deg)	δ_r (deg)	i_t (deg)					
149	Complete model	Landing	$P_{1R}P_{2R}$	27.1	0	0	0	1.5	4.9		[e]Take-off power	4.09	18
150	---- do -----	--- do ---	- do-	27.1	0	0	0	1.5		6.8	- do--	4.09	16
151	---- do -----	--- do ---	- do-	27.1	0	0	0	1.5	-5		- do--	4.09	18
152	Wing+fuselage	--- do ---	- do-	27.1	0				-5		- do--	4.09	14
153	---- do -----	--- do ---	- do-	27.1	0					6.8	- do--	4.09	12
154	---- do -----	--- do ---	- do-	27.1	0				5		- do--	4.09	14
155	---- do -----	--- do ---	$P_{1L}P_{2R}$	27.1	0				5		- do--	4.09	14
156	---- do -----	--- do ---	- do-	27.1	0					6.8	- do--	4.09	12
157	---- do -----	--- do ---	- do-	27.1	0				-5		- do--	4.09	14
158	---- do -----	--- do ---	$P_{1R}P_{2L}$	27.1	0				-5		- do--	4.09	14
159	---- do -----	--- do ---	- do-	27.1	0					6.8	- do--	4.09	12
160	---- do -----	--- do ---	- do-		0				5		- do--	4.09	14
161	Wing alone	--- do ---	- do-	27.1	0				5		- do--	4.09	10
162	---- do -----	--- do ---	- do-	27.1	0					6.8	- do--	4.09	8
163	---- do -----	--- do ---	- do-	27.1	0				-5		- do--	4.09	10
164	---- do -----	--- do ---	$P_{1L}P_{2R}$	27.1	0				-5		- do--	4.09	10
165	---- do -----	--- do ---	- do-	27.1	0					6.8	- do--	4.09	8
166	---- do -----	--- do ---	- do-	27.1	0				5		- do--	4.09	10
167	---- do -----	--- do ---	$P_{1R}P_{2R}$	27.1	0				5		- do--	4.09	10
168	---- do -----	--- do ---	- do-	27.1	0					6.8	- do--	4.09	8
169	---- do -----	--- do ---	- do-	27.1	0				-5		- do--	4.09	10
170	Complete model	High-speed	$P_{1R}P_{2L}$	27.1	0	0	0	1.5	0	0.6	Thrust calibration	4.09	5
171	---- do -----	Landing			0	0	0	1.5	4.9		No propellers	4.09	18
172	---- do -----	--- do ---			0	0	0	1.5		6.8	- do--	4.09	16
173	---- do -----	--- do ---			0	0	0	1.5	-4.9		- do--	4.09	18
174	Wing+fuselage	--- do ---			0				5		- do--	4.09	14
175	---- do -----	--- do ---			0					6.8	- do--	4.09	12
176	---- do -----	--- do ---			0				-5		- do--	4.09	14
177	[f]Wing alone	--- do ---			0				5		- do--	4.09	10
178	---- do -----	--- do ---			0					6.8	- do--	4.09	8
179	---- do -----	--- do ---			0				-5		- do--	4.09	10
180	[g]Wing alone	--- do ---	$P_{1R}P_{2R}$	27.1	0				-5		[e]Take-off power	4.09	10
181	---- do -----	--- do ---	- do-	27.1	0					6.8	- do--	4.09	8
182	---- do -----	--- do ---	- do-	27.1	0				5		- do--	4.09	10
183	Wing alone	High-speed	$P_{1L}P_{2R}$	40.5	0				0	-4.8	Thrust calibration	16.37	19, 20
184	---- do -----	--- do ---	- do--	40.5	0				0	8.0	- do--	16.37	19, 20
185	---- do -----	--- do ---	$P_{1R}P_{2L}$	40.5	0				0	-4.8	- do--	16.37	19, 20
186	---- do -----	--- do ---	- do--	40.5	0				0	8.0	- do--	16.37	19, 20

[a]Definition of symbols:

P_{1R} left-hand motor, right-hand propeller

P_{2R} right-hand motor, right-hand propeller

P_{1L} left-hand motor, left-hand propeller

P_{2L} right-hand motor, left-hand propeller

[b]Range of values indicated when numerical values are omitted.
[e]2000 hp at sea level.
[f]Without center-section split flaps.
[g]With center-section split flaps.

NACA

Fig. 1

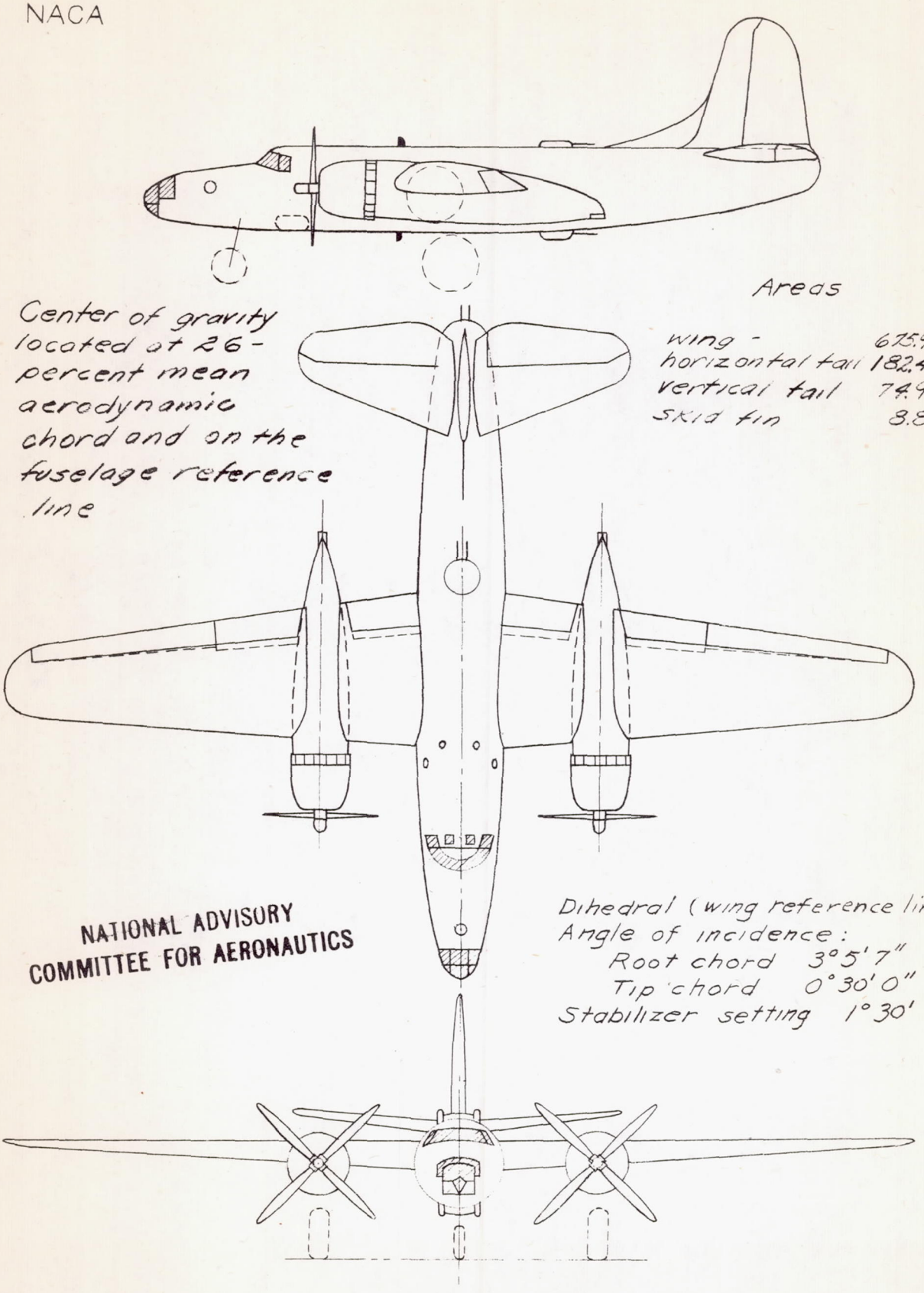

FIGURE 1. - Three-view drawing of the North American XB-28 airplane.

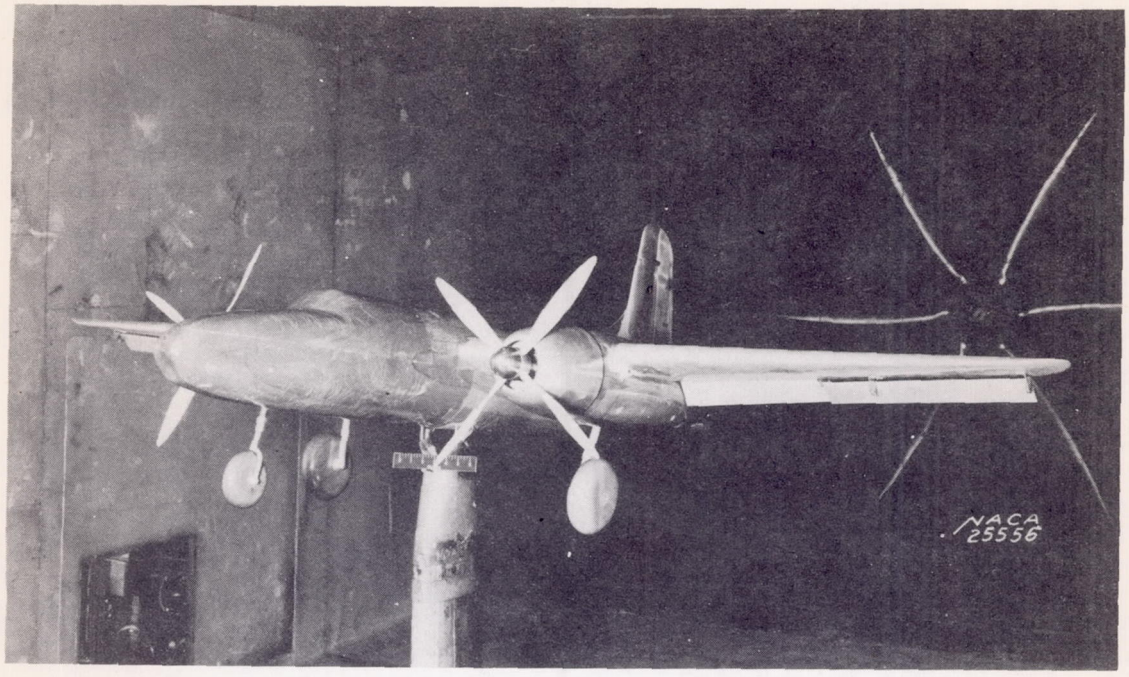

Figure 2a.- Three-quarter front view of the 1/10-scale model of the North American XB-28 airplane.

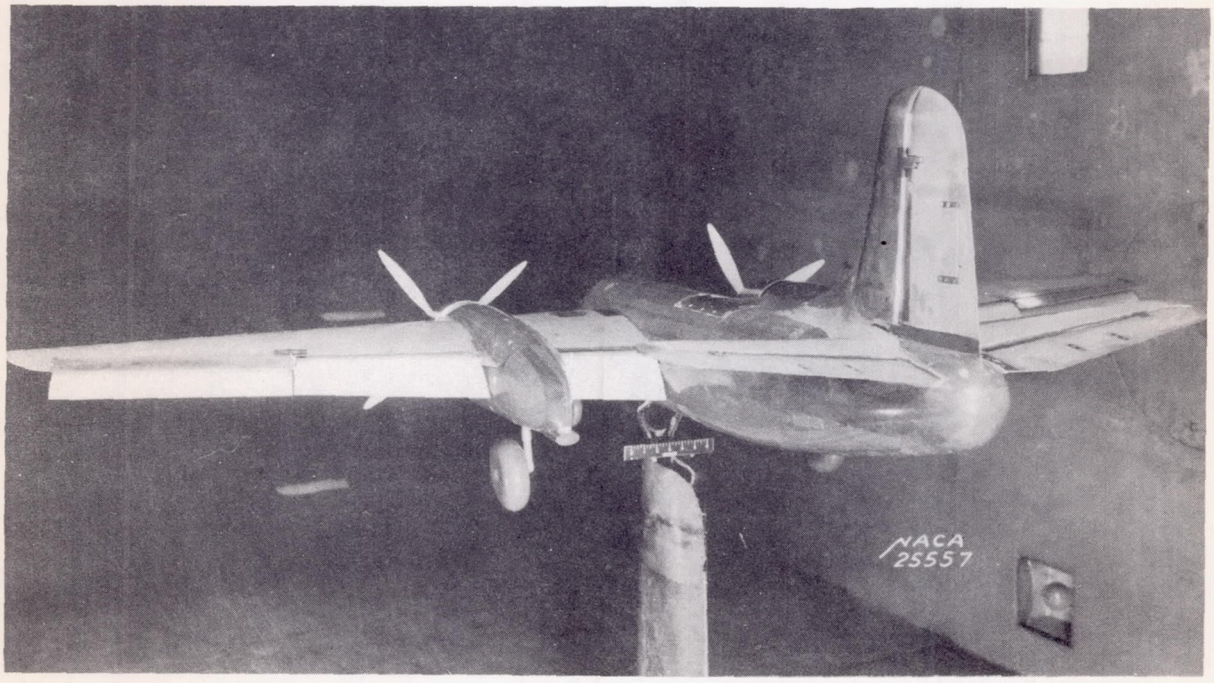

Figure 2b.- Three-quarter rear view of the 1/10-scale model of the North American XB-28 airplane mounted in the 7- by 10-foot wind tunnel. Horizontal tail $H_7$7.5 duplex flaps deflected, landing gear extended, and propellers on.

L-295

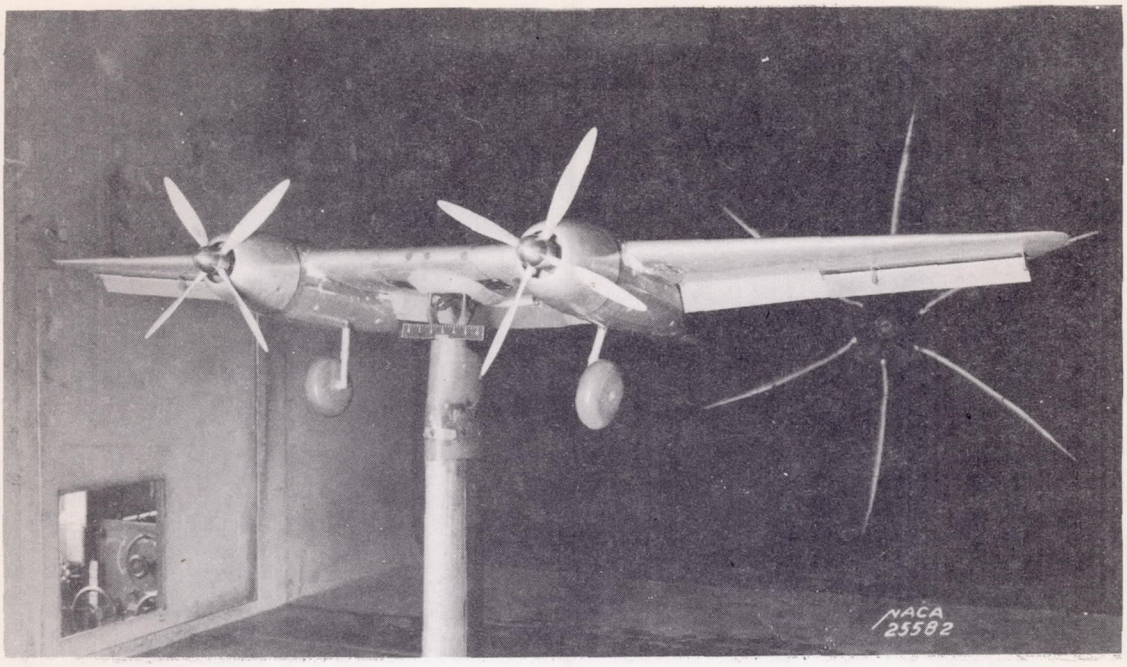

Figure 3a.- Three-quarter front view of the wing of the 1/10-scale model of the North American XB-28 airplane in the 7- by 10-foot wind tunnel. Wing with duplex flaps deflected (split flap over center section normally covered by fuselage), landing gear extended, and propellers on.

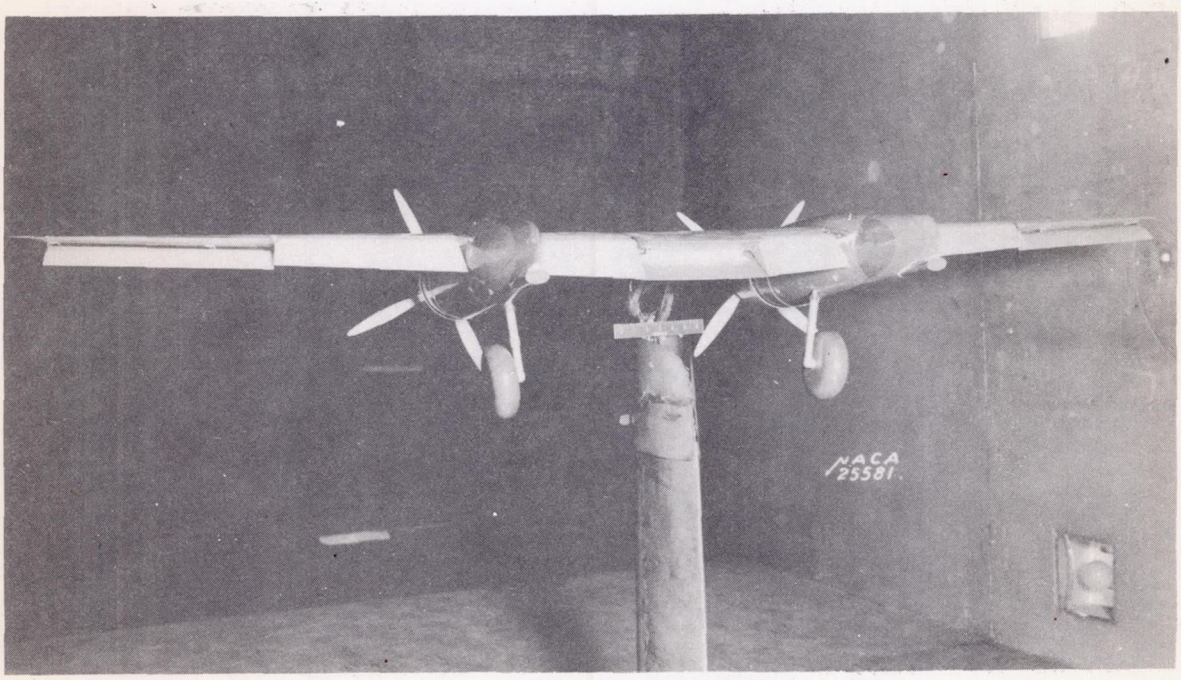

Figure 3b.- Three-quarter rear view of the wing of the 1/10-scale model of the North American XB-28 airplane in the 7- by 10-foot wind tunnel. Wing with duplex flaps extended (split flap over center section normally covered by fuselage), landing gear extended, and propellers on.

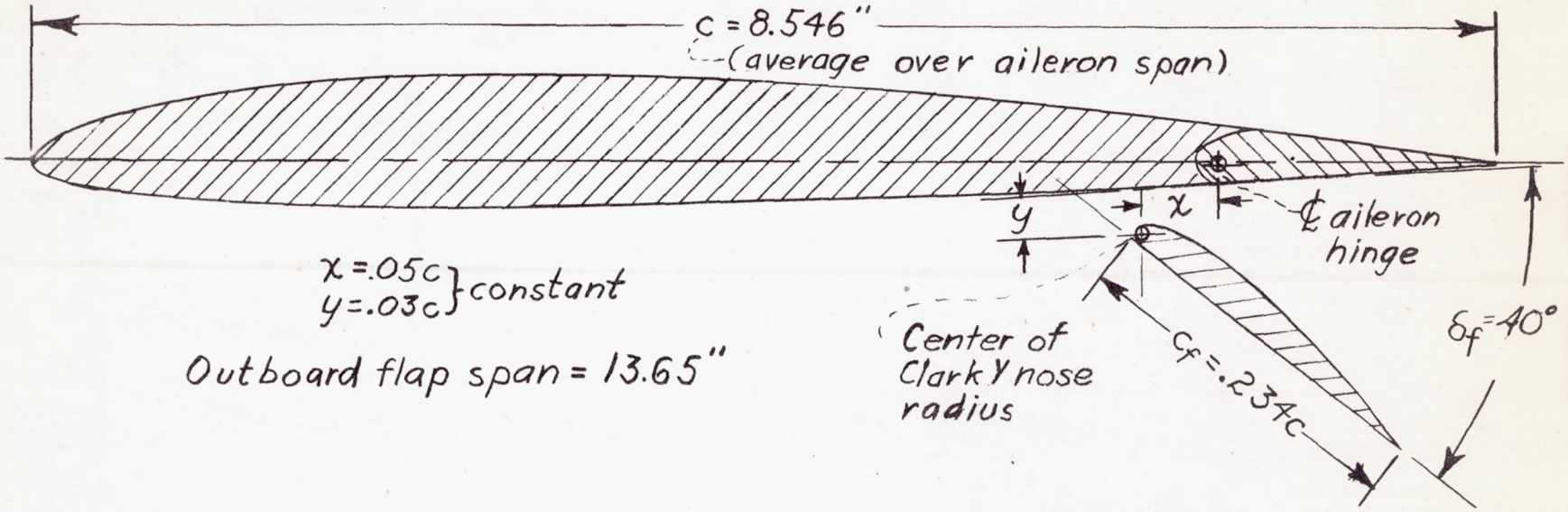

Figure 4.— Typical section of the outboard flap of the duplex flap arrangement on the 1/10-scale model of the North American XB-28 airplane.

NACA (Measure with 5/16") Fig. 5a

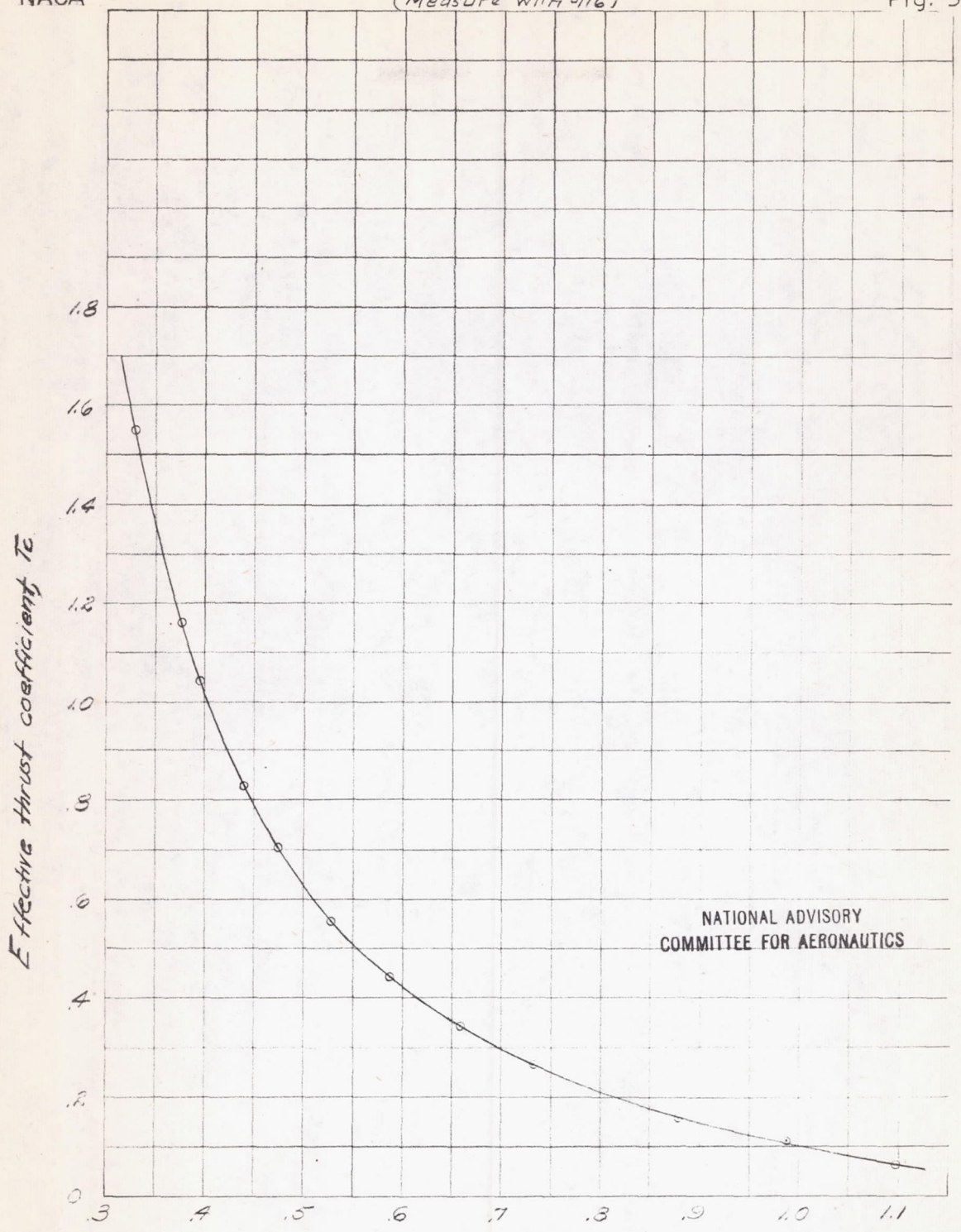

(a) $\beta_{.8}$, 27.1°; propeller rotation mode P_{1R} P_{2L}; d_w, 0.6°; δ_e, δ_r, δ_a, δ_t, 0°; tunnel velocity, 61.0 feet per second. Test 170.

Figure 5.- Effective-thrust-coefficient calibration of propellers of 1/10-scale model of North American XB-28 airplane.

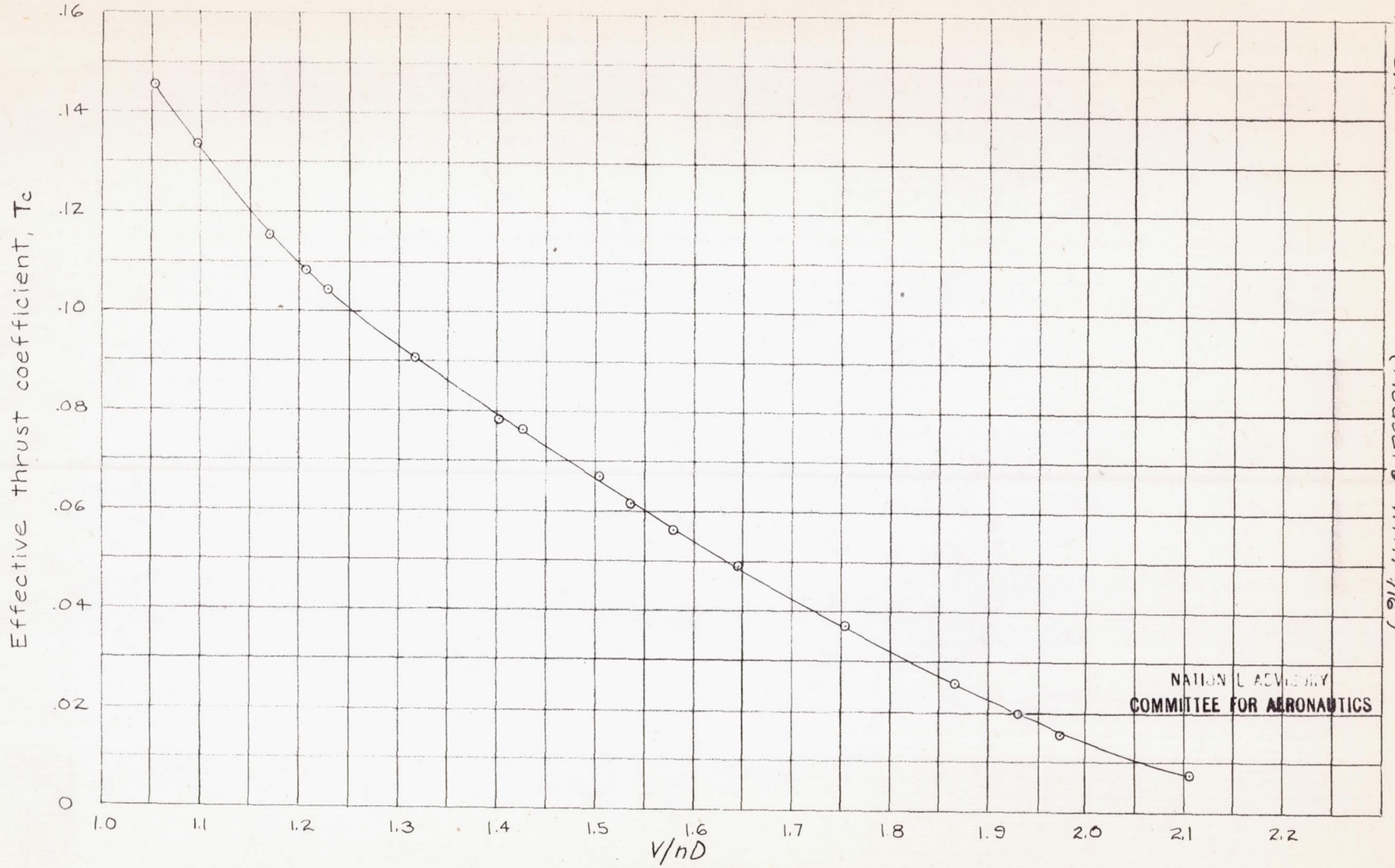

(b) β_s 40.5°; propeller rotation mode $P_R P_{RR}$; $\alpha_u = 0.6°$; δ_a, δ_e, δ_r, δ_f, 0°; tunnel velocity, 121.9 feet per second. Test 68a.

Figure 5.- Concluded.

Fig. 5b

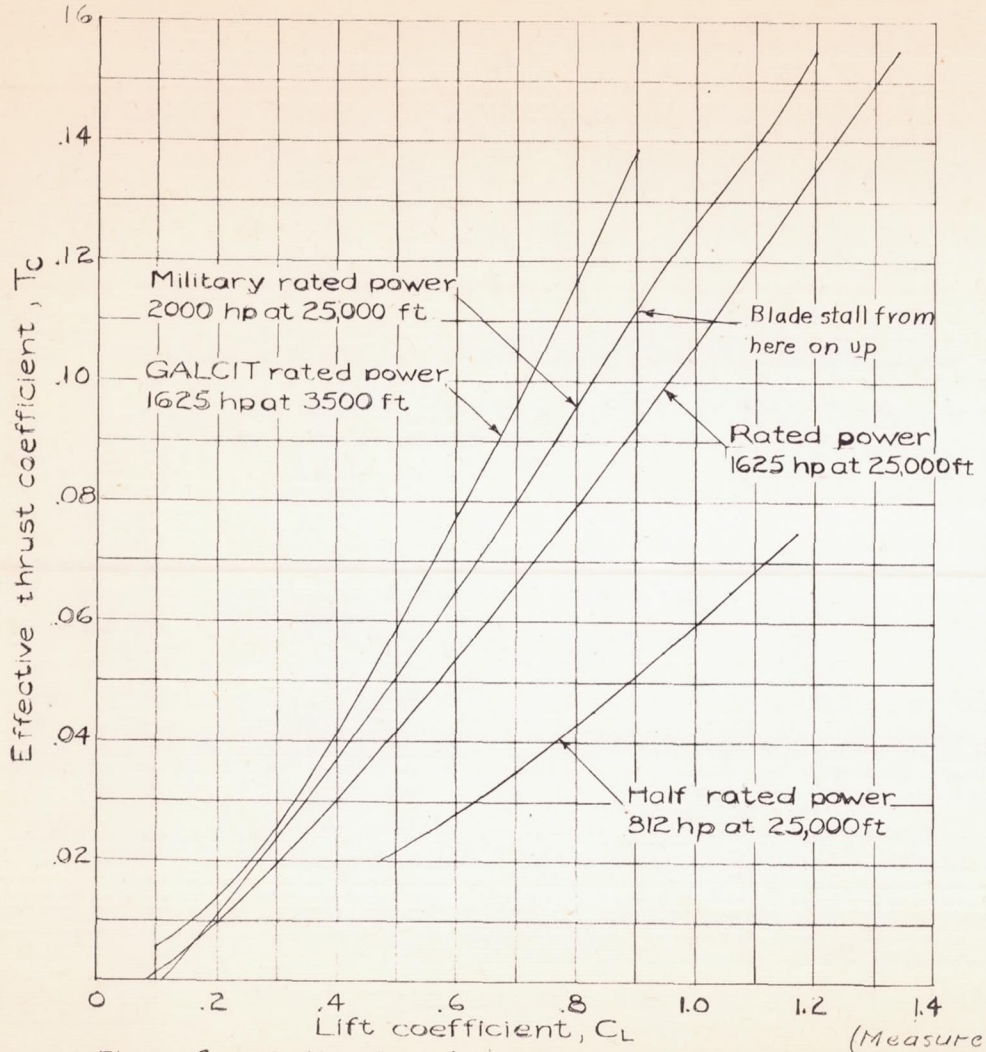

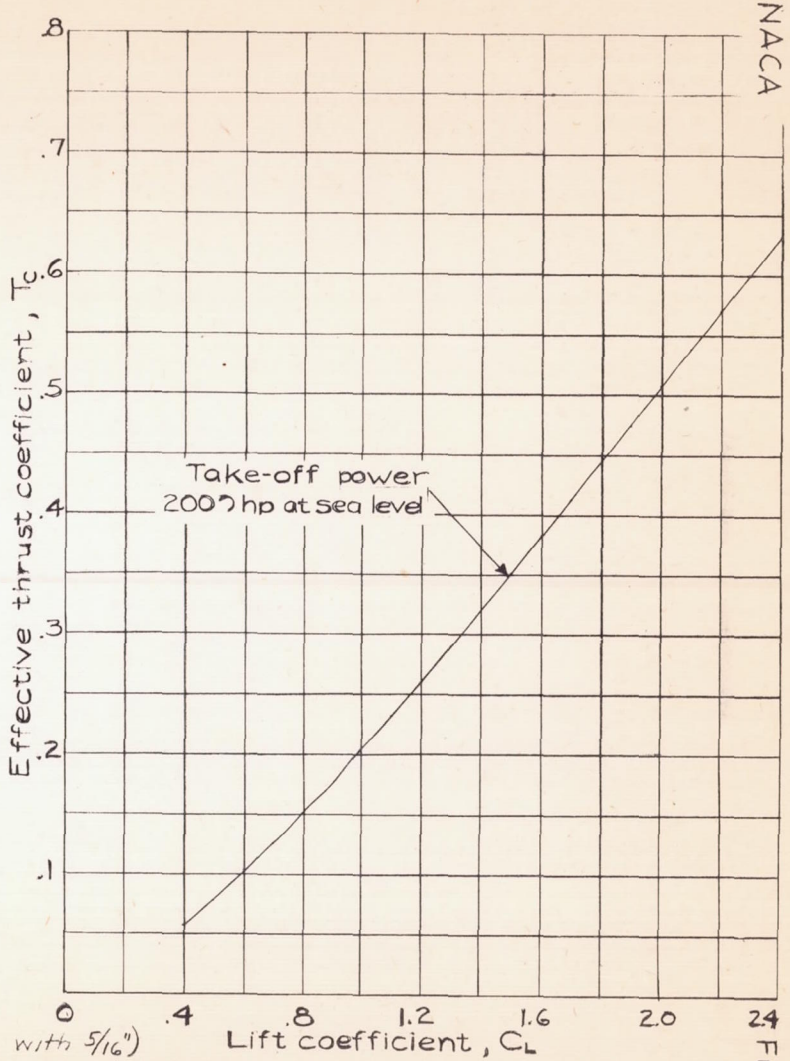

(Measure with 5/16")

FIGURE 6.- Effective thrust coefficients for the power conditions simulated in the tests of the $\frac{1}{10}$-scale model of the North American XB-28 airplane.

NACA

Fig. 6

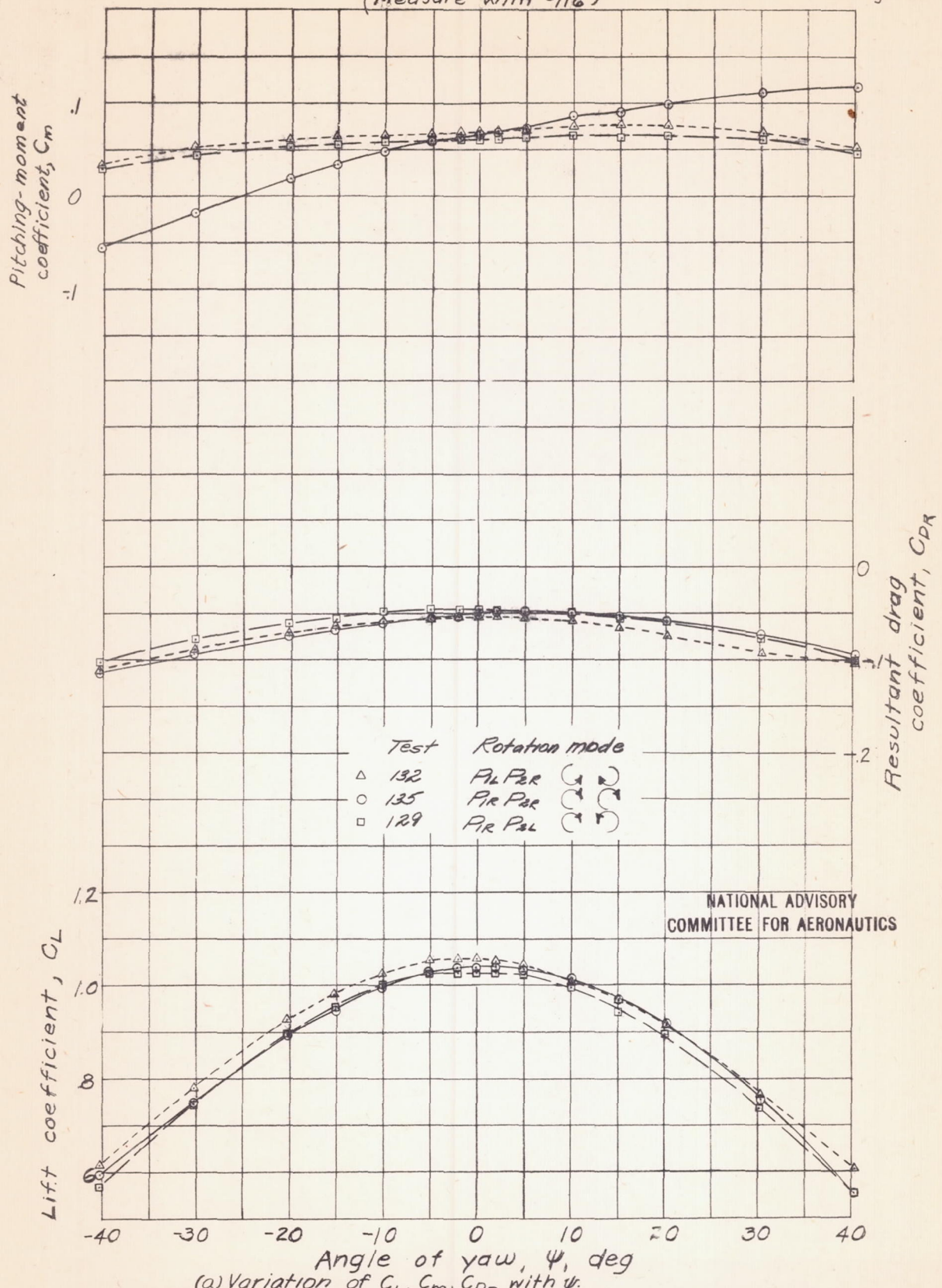

(a) Variation of C_L, C_m, C_{D_R} with ψ.

FIGURE 7.- Effect of propeller rotation on the aerodynamic characteristics in yaw of the wing of the 1/10-scale model of the North American XB-28 airplane. High-speed condition; landing gear up; cowl flaps closed; rated power; β, 40.5°; δ_a, δ_f, 0°; q, 16.37 pounds per square foot.

L-295

NACA (Measure with 5/16") Fig. 7b

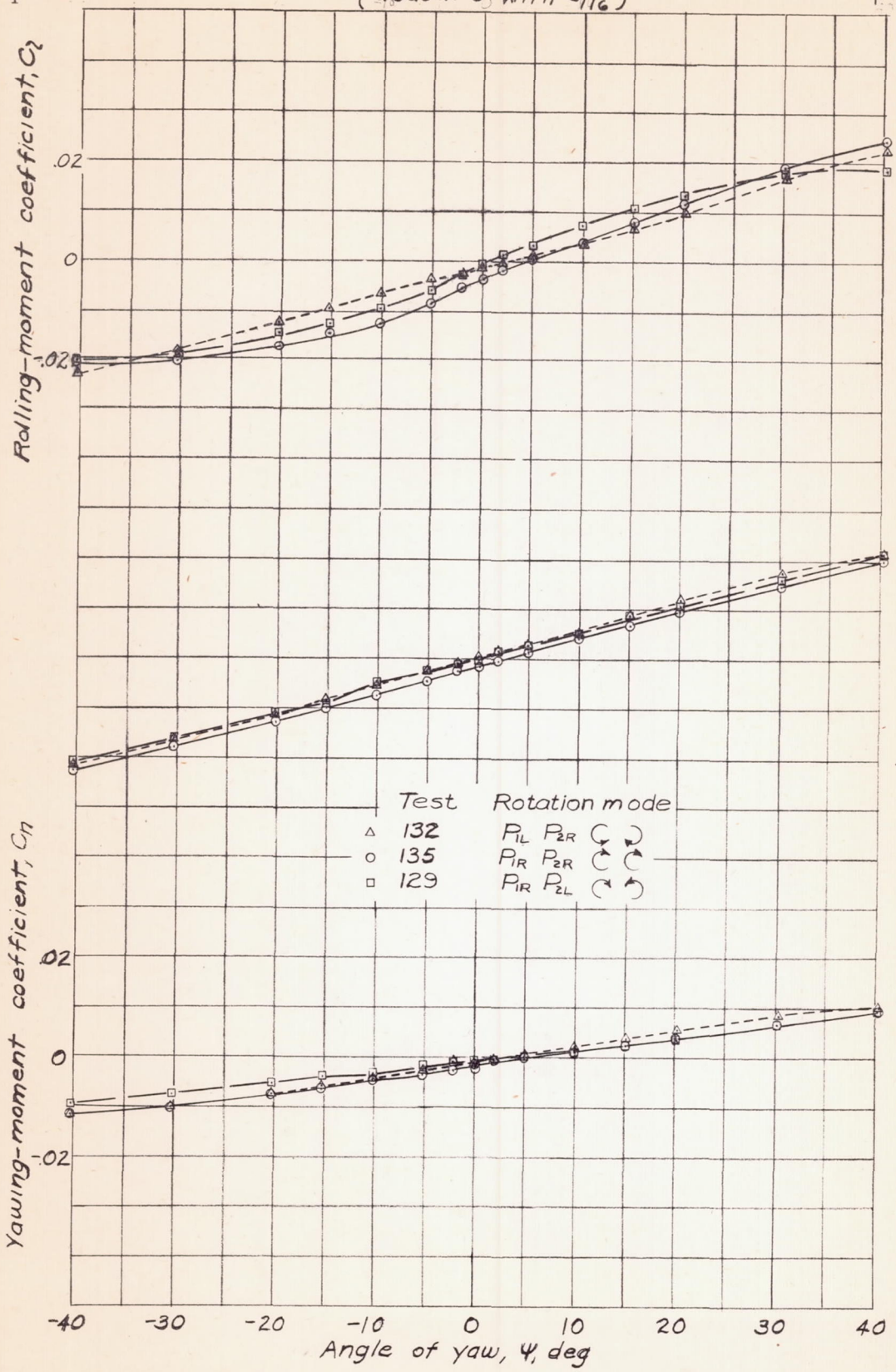

(b) Variation of C_n, C_l, and C_y with ψ.

FIGURE 7.- Concluded.

L-295

NACA

(Measure with 5/16")

Fig. 8a

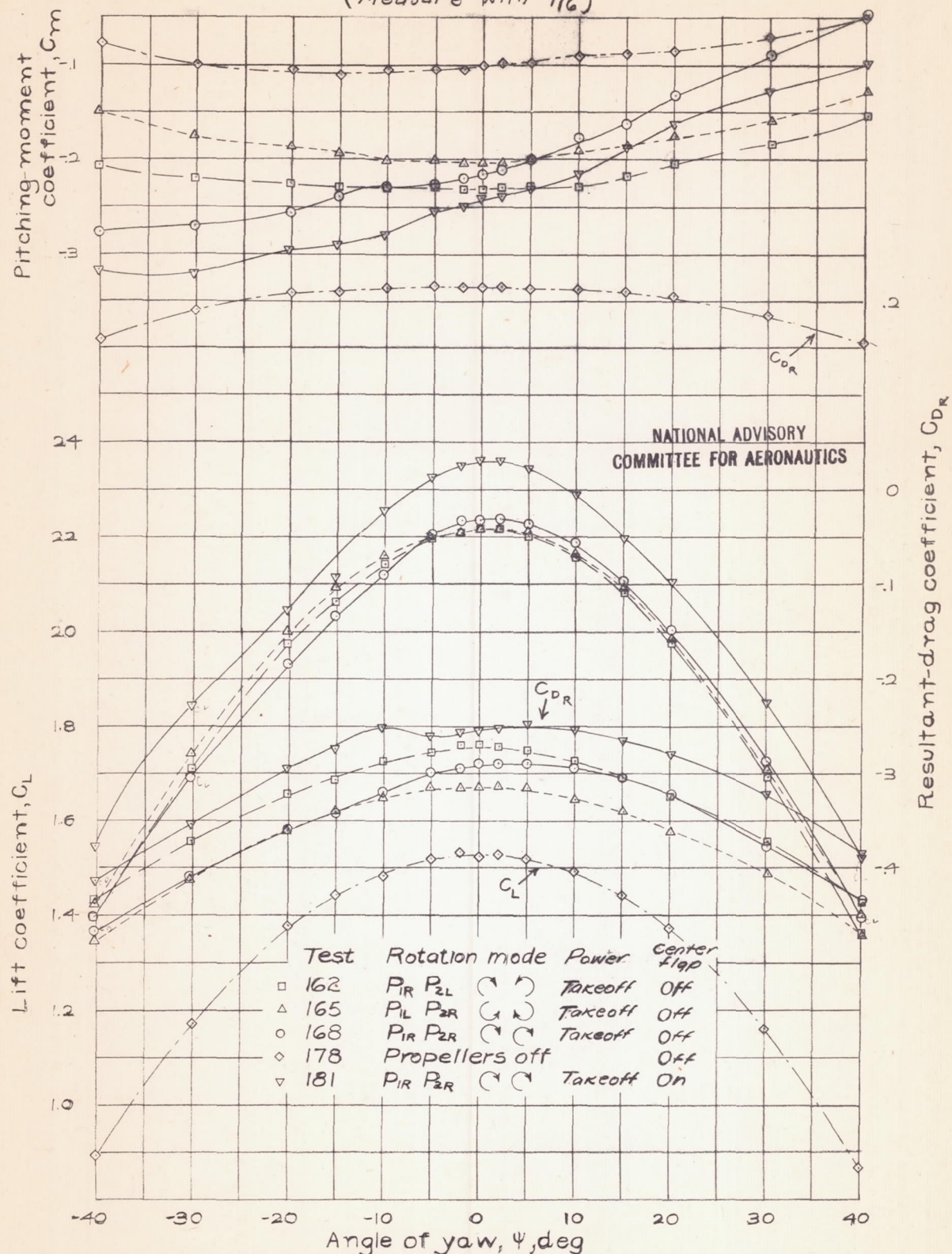

(a) Variation of C_L, C_m, and C_{D_R} with ψ.

FIGURE 8.- Effect of propeller rotation, power, and center section flap on the aerodynamic characteristics in yaw of the wing of the 1/10-scale model of the North American XB-28 airplane. Landing condition; landing gear down; cowling flaps closed; β, 27.1°; δ_{f_1}, 45°; δ_{f_2}, 40°; q, 4.09 pounds per square foot.

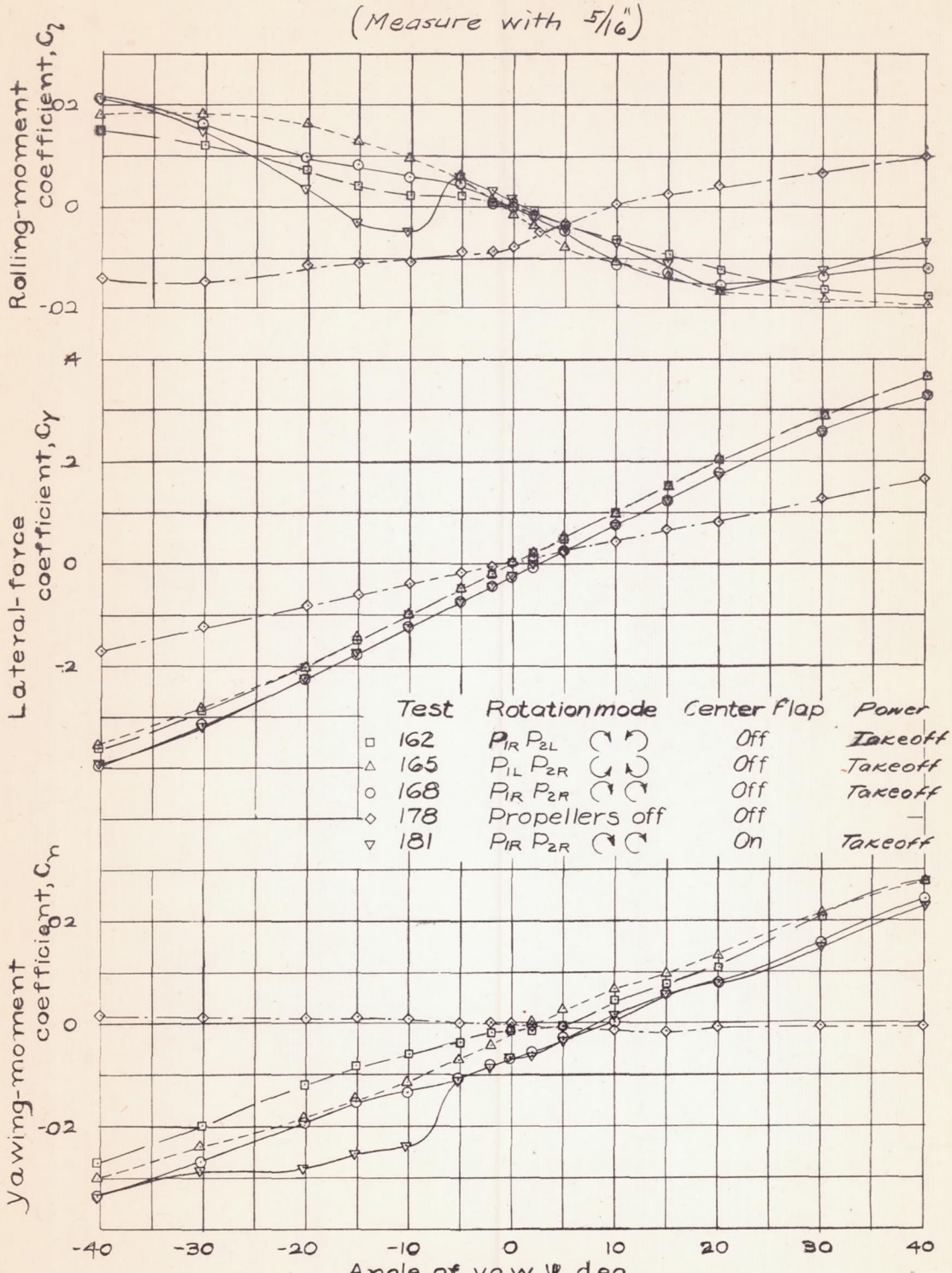

(b) Variation of C_n, C_l, and C_y with ψ.

FIGURE 8.- Concluded.

NACA

Fig. 9a

(Measure with 5/16")

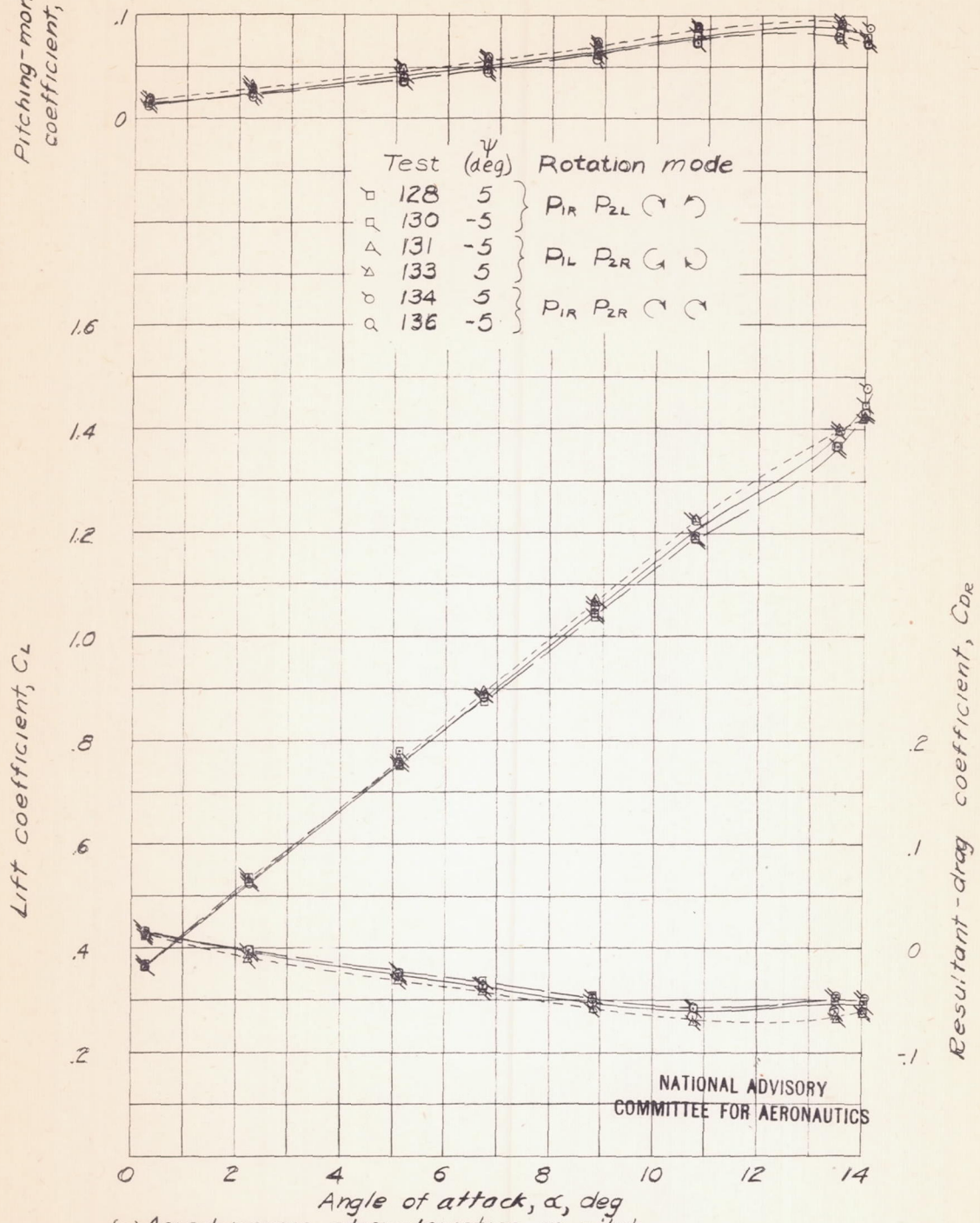

(a) Aerodynamic characteristics in pitch.

FIGURE 9.- Effect of propeller rotation on the aerodynamic characteristics of the wing of the 1/10-scale model of the North American XB-28 airplane. High-speed condition; landing gear up; cowl flaps closed; rated power; β, 40.5°; δ_a, δ_f, 0°; q, 16.37 pounds per square foot.

(Measure with 5/16")

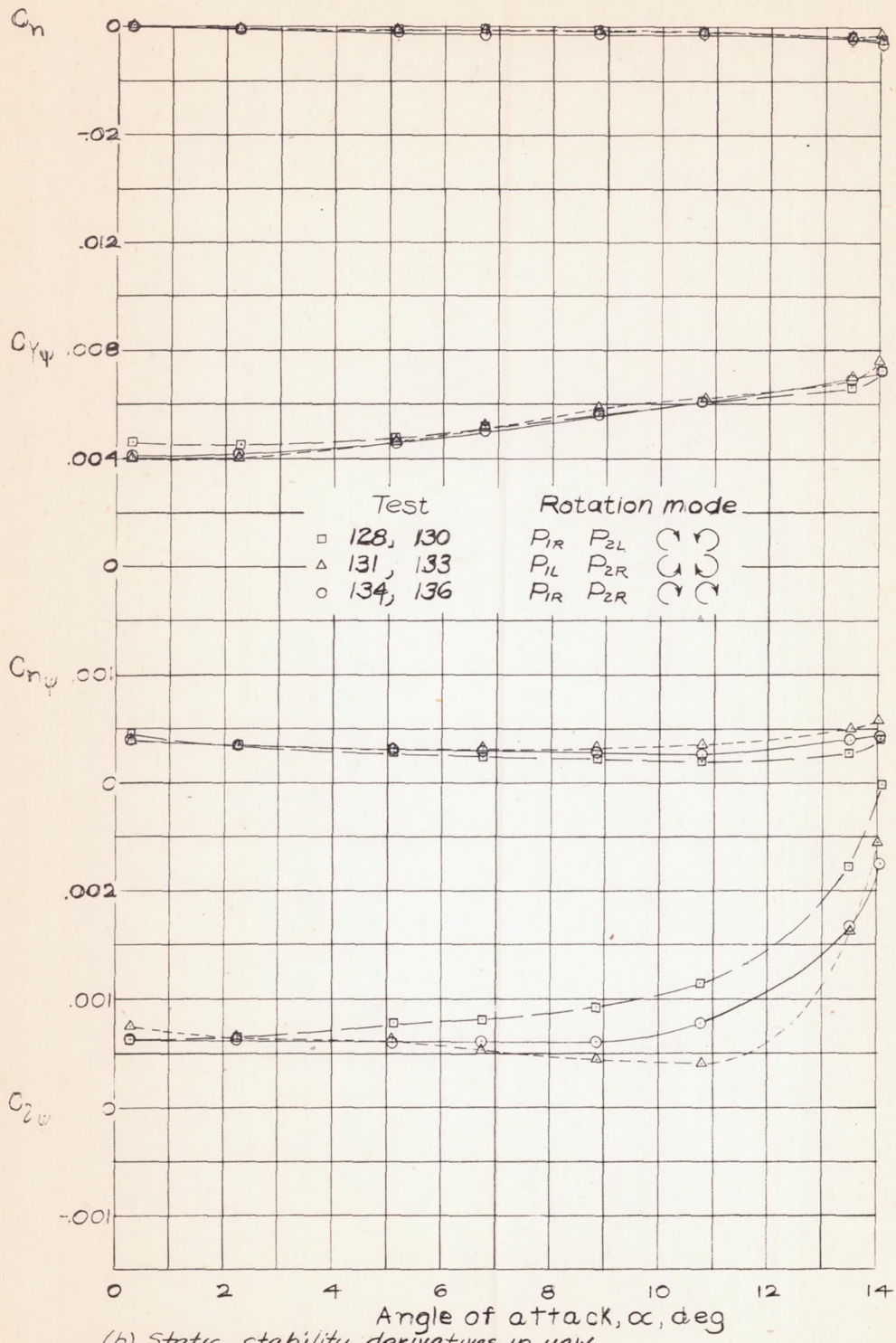

(b) Static-stability derivatives in yaw.

FIGURE 9.- Concluded.

NACA

Fig. 10a

NATIONAL ADVISORY
COMMITTEE FOR AERONAUTICS

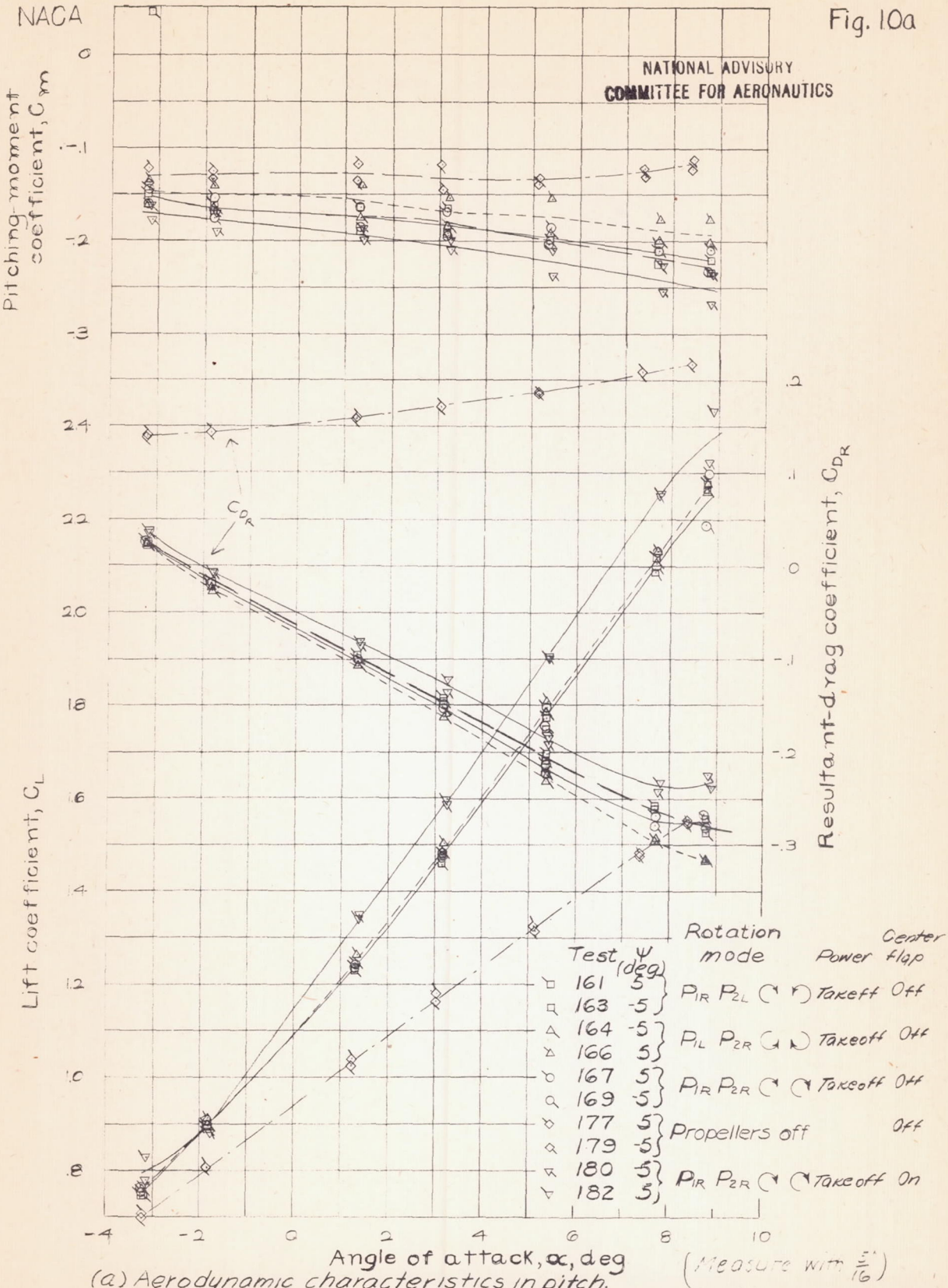

(Measure with $\frac{5}{16}$)

(a) Aerodynamic characteristics in pitch.

FIGURE 10.- Effect of propeller rotation, power, and center-section flap on the aerodynamic characteristics of the wing of the 1/10-scale model of the North American XB-28 airplane. Landing condition; landing gear down; cowl flap closed; β, 27.1°; δ_{f_1}, 45°; δ_{f_2}, 40°; q, 4.09 pounds per square foot.

(Measure with 5/16")

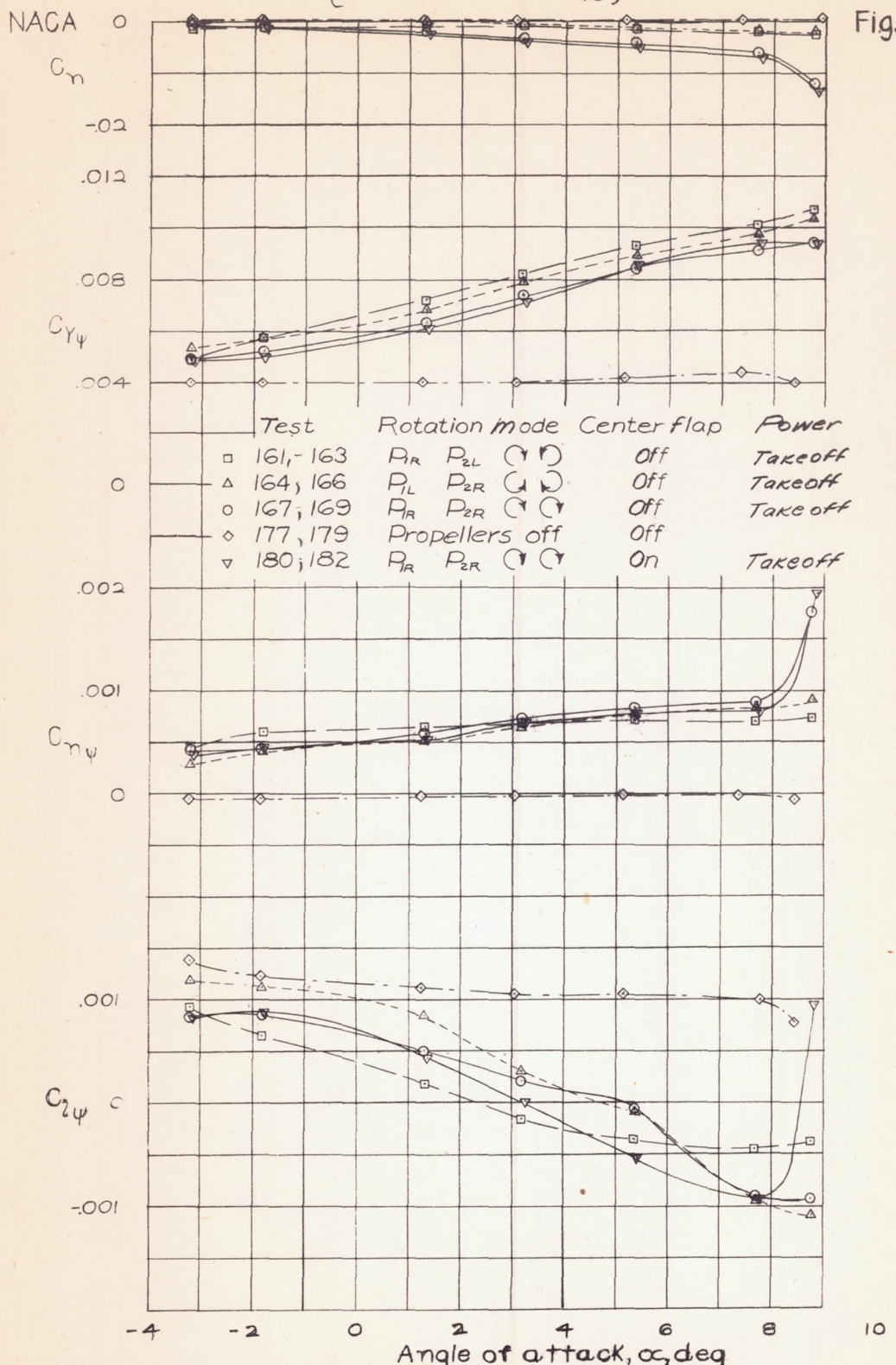

Fig. 10b

(b) Static-stability derivatives in yaw.

Figure 10.- Concluded.

NACA (Measure with 5/16")

Fig. 11a

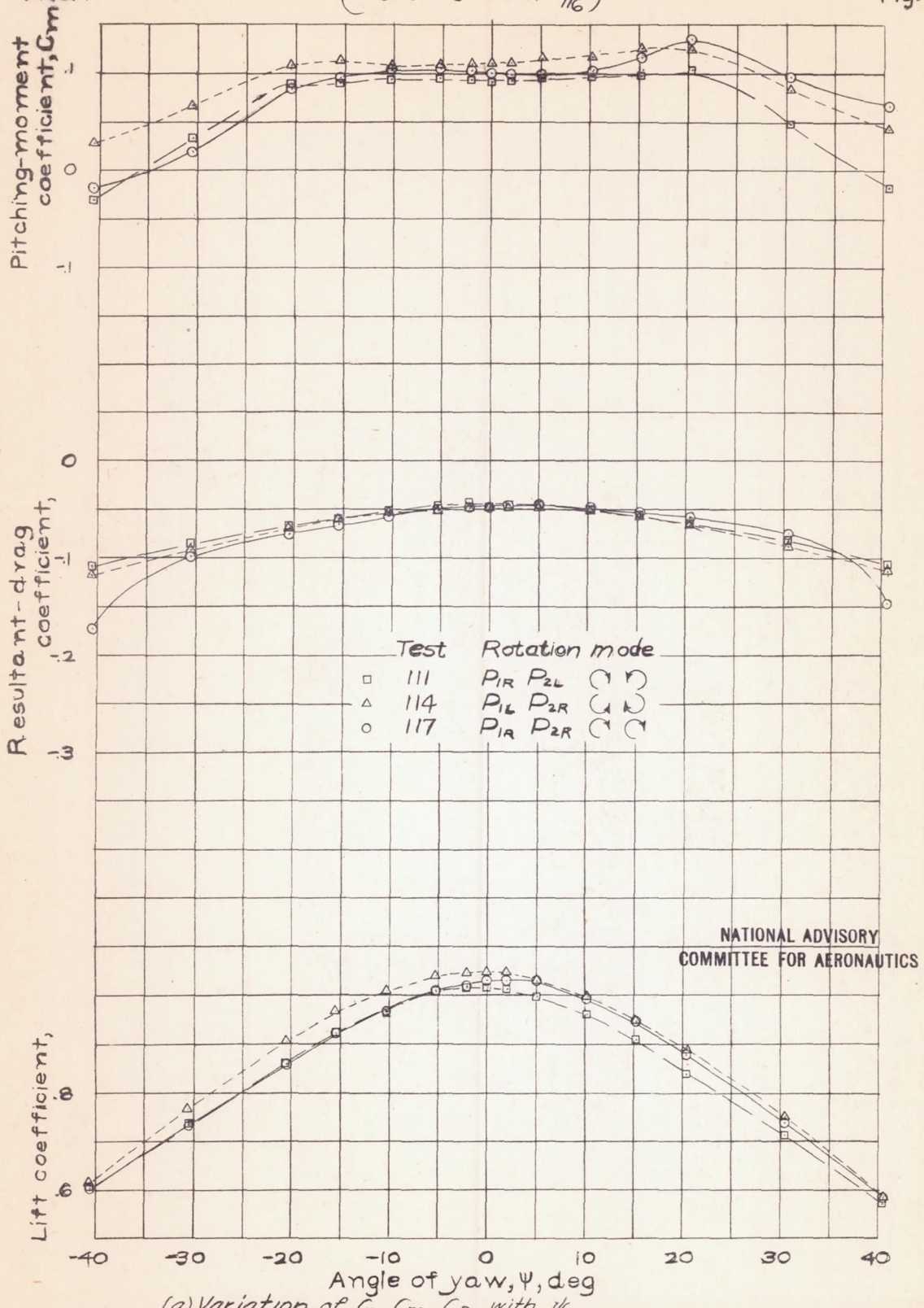

(a) Variation of C_L, C_m, C_{D_R} with ψ.

FIGURE 11.- Effect of propeller rotation on the aerodynamic characteristics in yaw of the wing plus fuselage of the 1/10-scale model of the North American XB-28 airplane. High-speed condition, landing gear up; cowl flaps closed; rated power; β, 40.5°; δ_a, δ_f, 0°; q, 16.37 pounds per square foot.

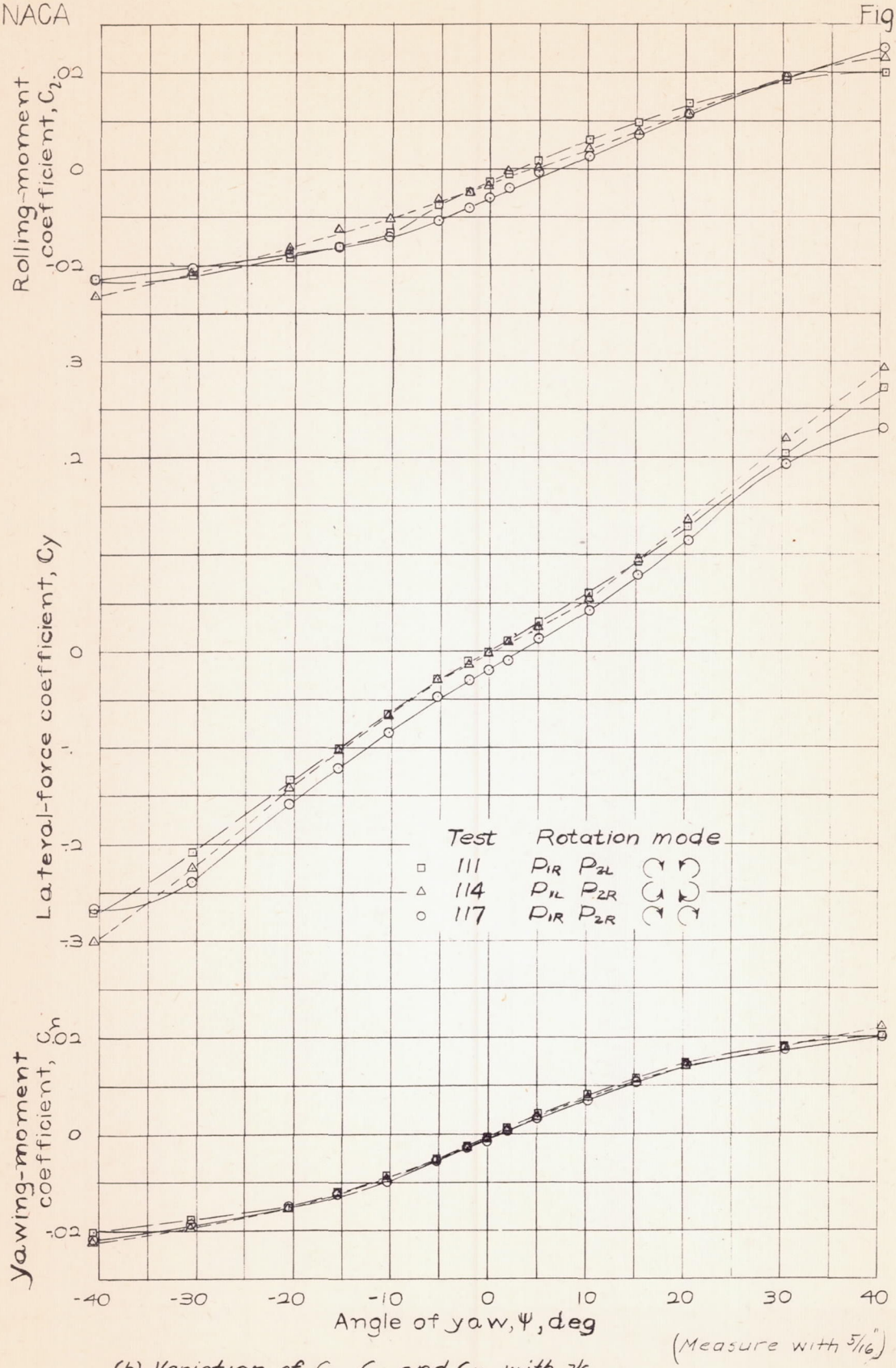

(b) Variation of C_n, C_l, and C_y with Ψ.

Figure 11.- Concluded.

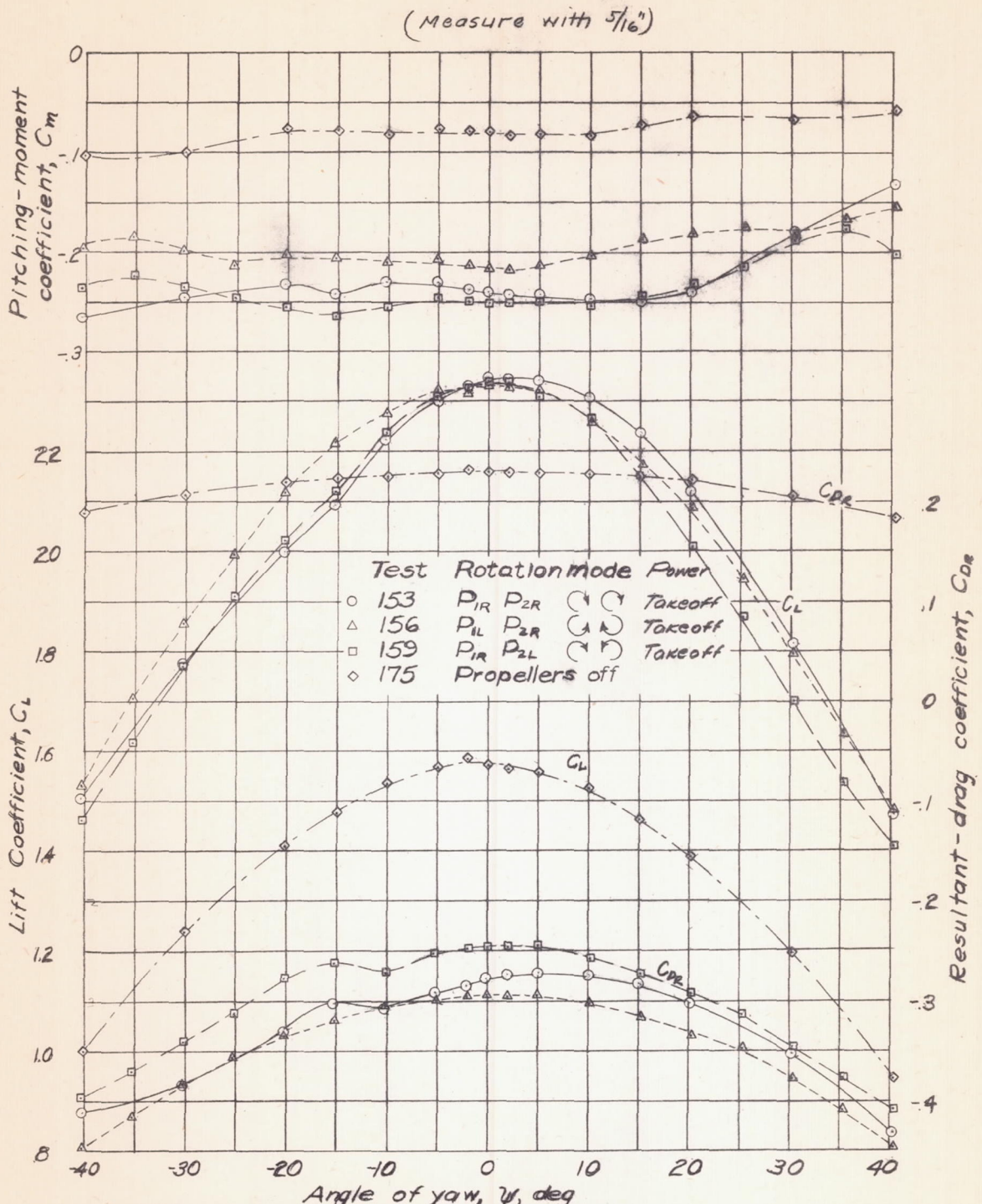

(a) Variation of C_L, C_m, and C_{D_R} with ψ.

Figure 12.- Effect of power and propeller rotation on the aerodynamic characteristics in yaw of wing plus fuselage of the 1/10-scale model of the North American XB-28 airplane. Landing condition; landing gear down; cowl flaps closed; β, 27.1°; δ_a, 0°; δ_{f_1}, 45°; δ_{f_2}, 40°; q, 40.9 pounds per square foot.

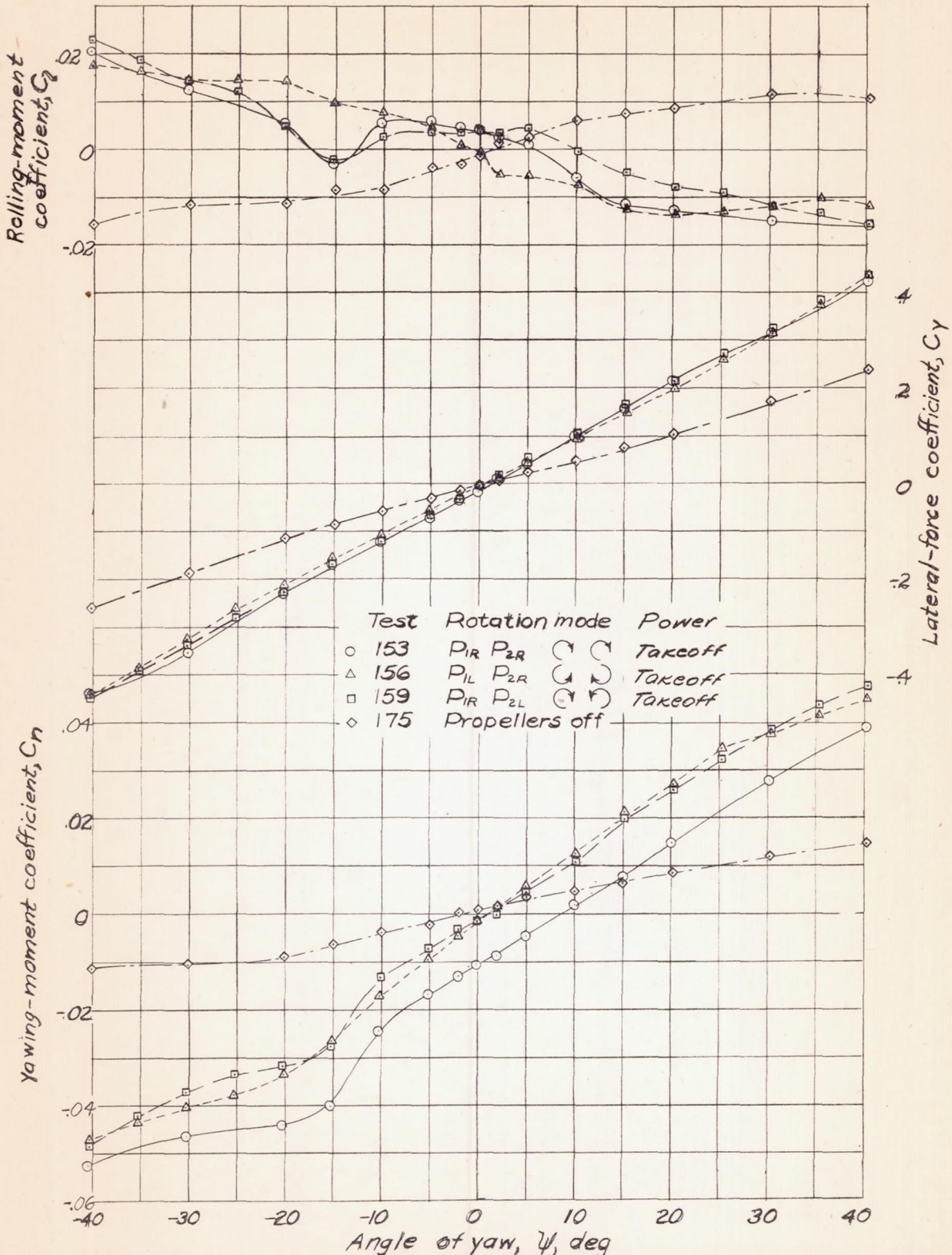

(b) Variation of C_n, C_l, and C_Y with ψ.

Figure 12.- Concluded.

(Measure with 5/16")

Fig. 13a

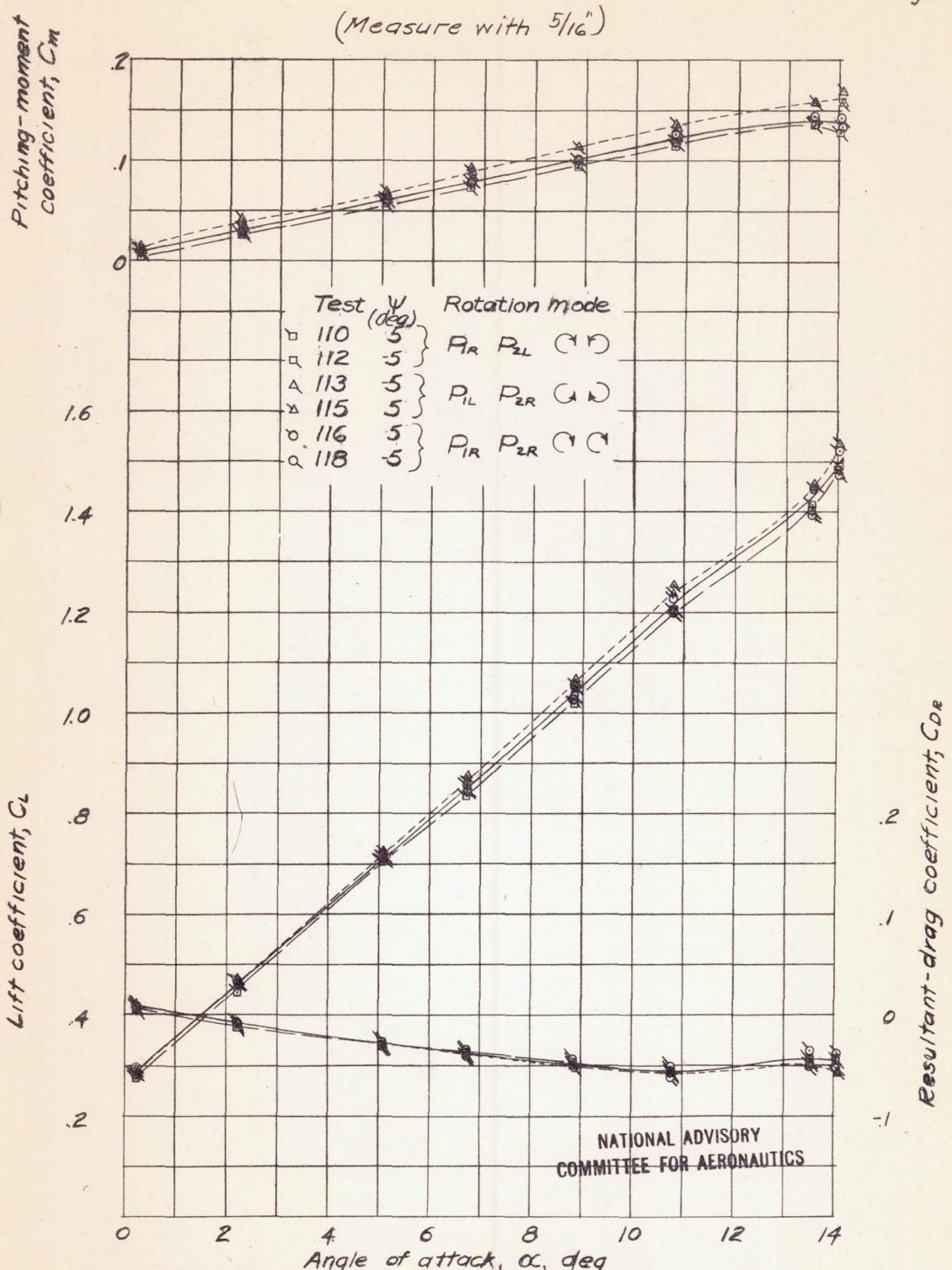

(a) Aerodynamic characteristics in pitch.

Figure 13.- Effect of propeller rotation on the aerodynamic characteristics of the wing plus fuselage of the 1/10-scale model of the North American XB-28 airplane. High-speed condition; landing gear up; cowl flaps closed; rated power; β, 40.5°; δ_a, δ_f, 0°; q, 16.37 pounds per square foot.

NACA

Fig. 13b

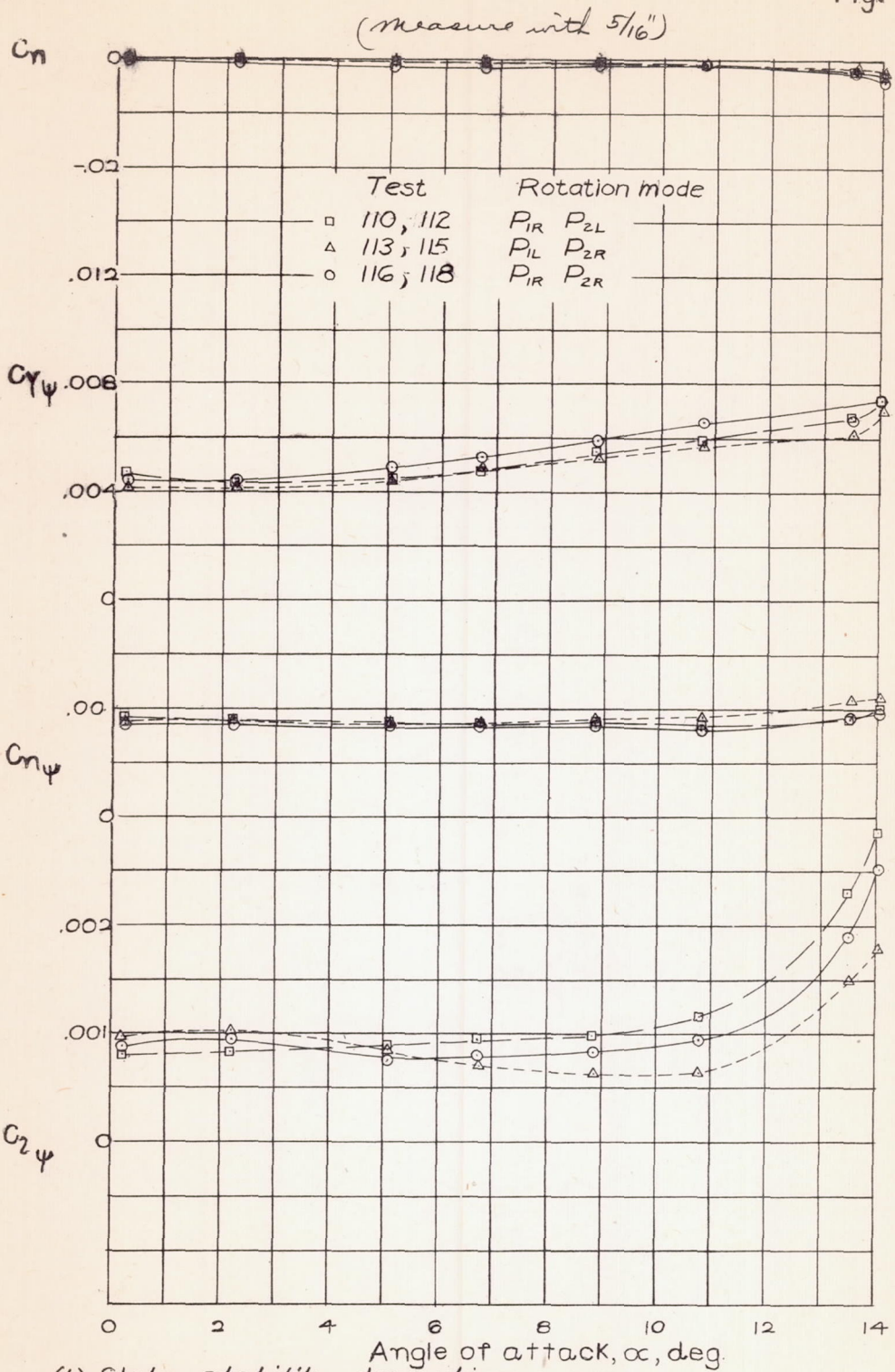

(b) Static-stability derivatives in yaw.

Figure 13.-Concluded.

NACA

Fig. 14a

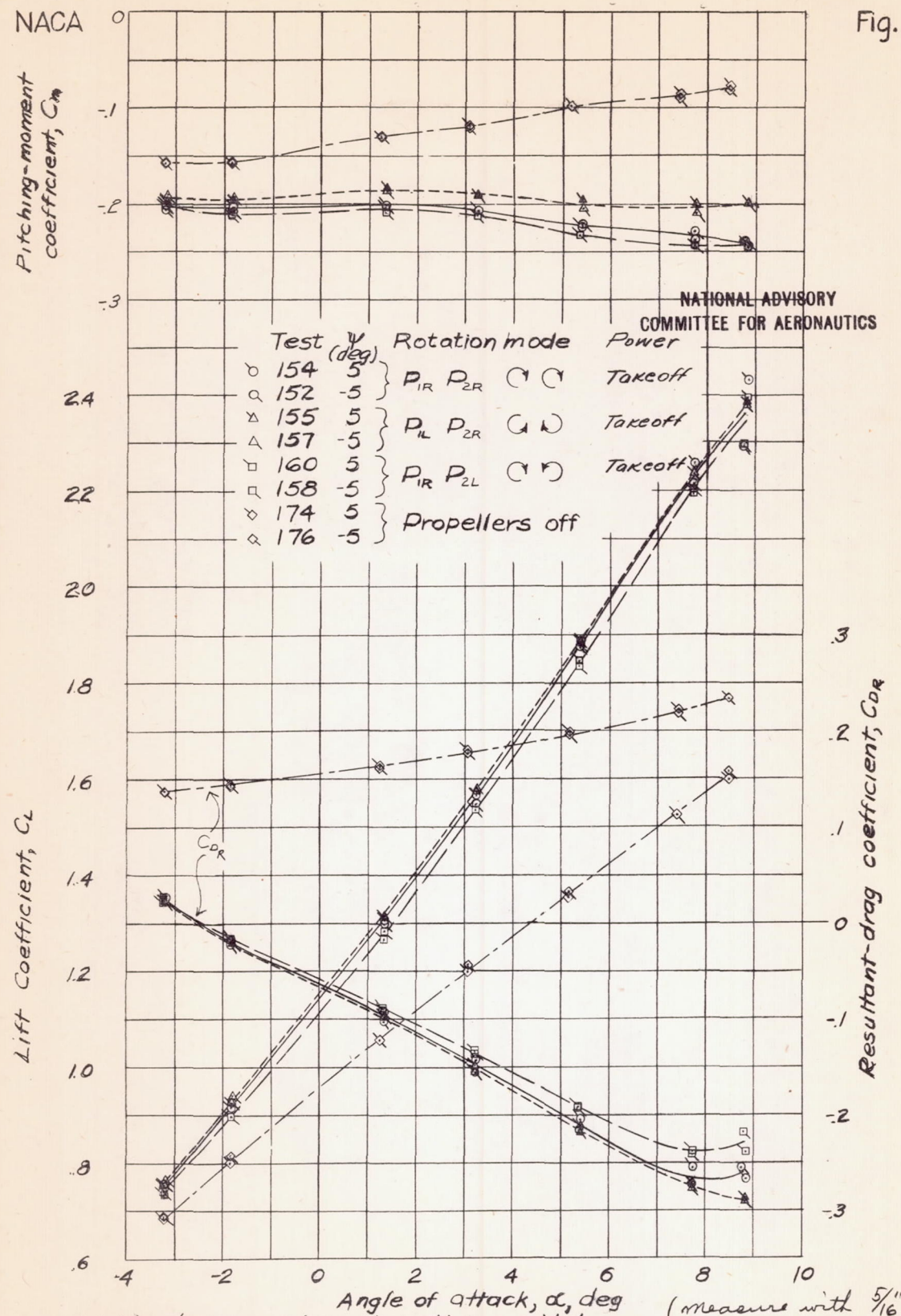

(a) Aerodynamic characteristics in pitch.

Figure 14.- Effect of power and propeller rotation on the aerodynamic characteristics of the wing plus fuselage of the 1/10-scale model of the North American XB-28 airplane. Landing condition; landing gear down; cowl flaps closed; β, 27.1°; δ_a, 0°; δ_{f_1}, 45°; δ_{f_2}, 40°; q, 4.09 pounds per square foot.

L-295

NACA

Fig. 14b

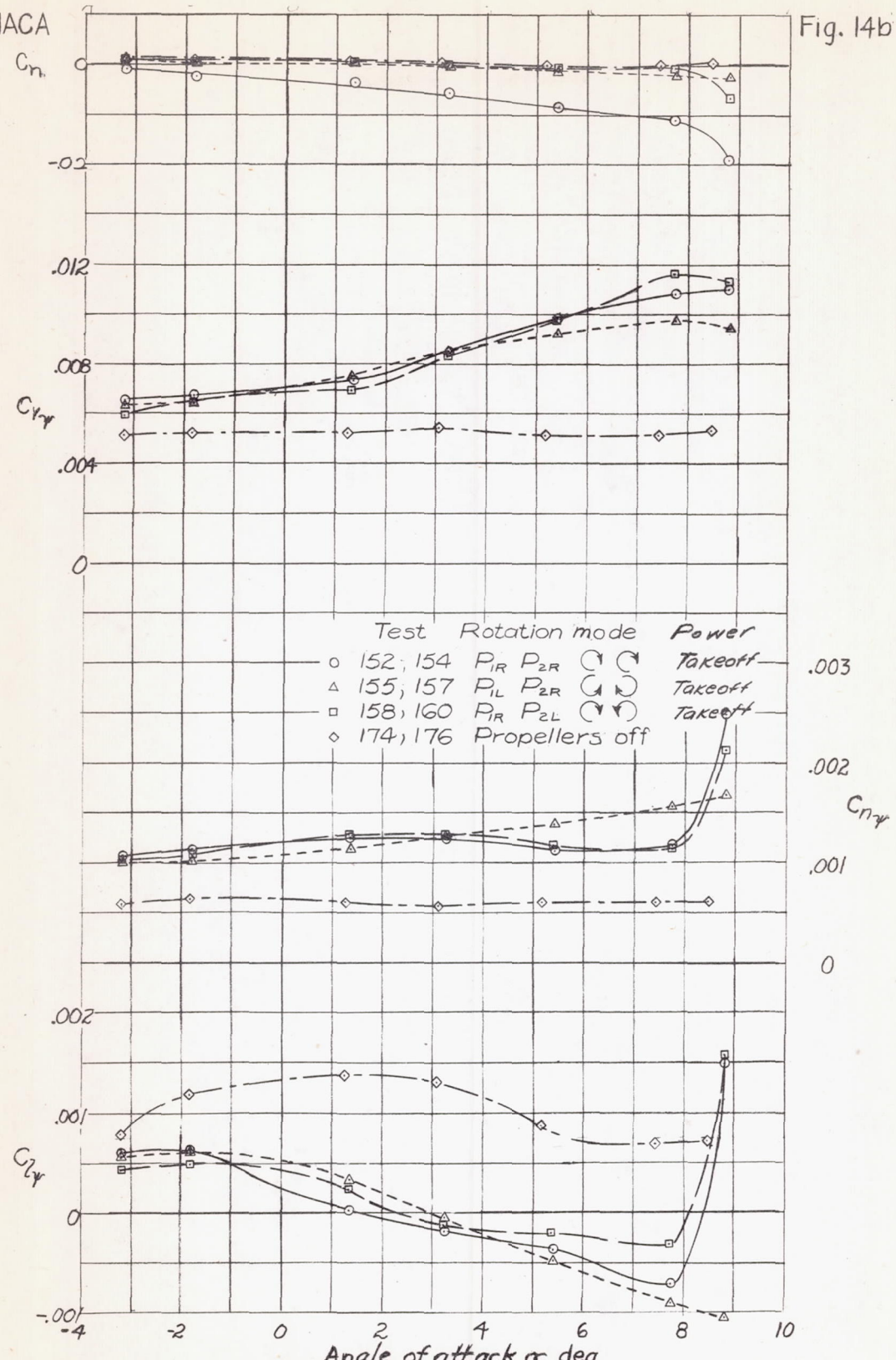

(b) Static-stability derivatives in yaw.

Figure 14. - Concluded.

(Measure with 5/16")

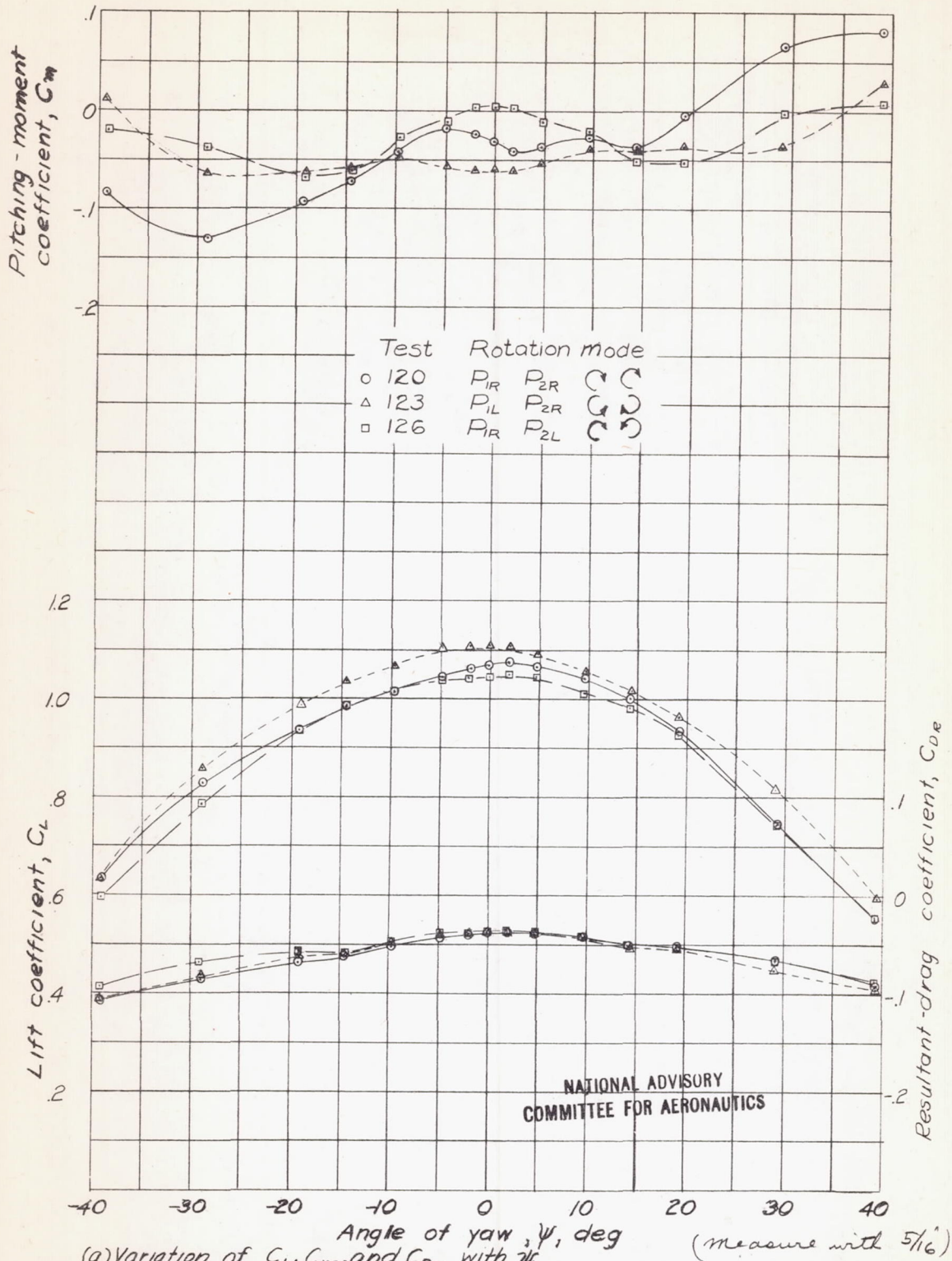

(a) Variation of C_L, C_m, and C_{D_R} with ψ.

Figure 15.- Effect of propeller rotation on the aerodynamic characteristics in yaw of the 1/10-scale complete model of the North American XB-28 airplane. High-speed condition; landing gear up; cowl flaps closed; rated power; β, 40.5°; δ_a, δ_f, δ_r, δ_e, 0°; q, 16.37 pounds per square foot.

NACA

Fig. 15b

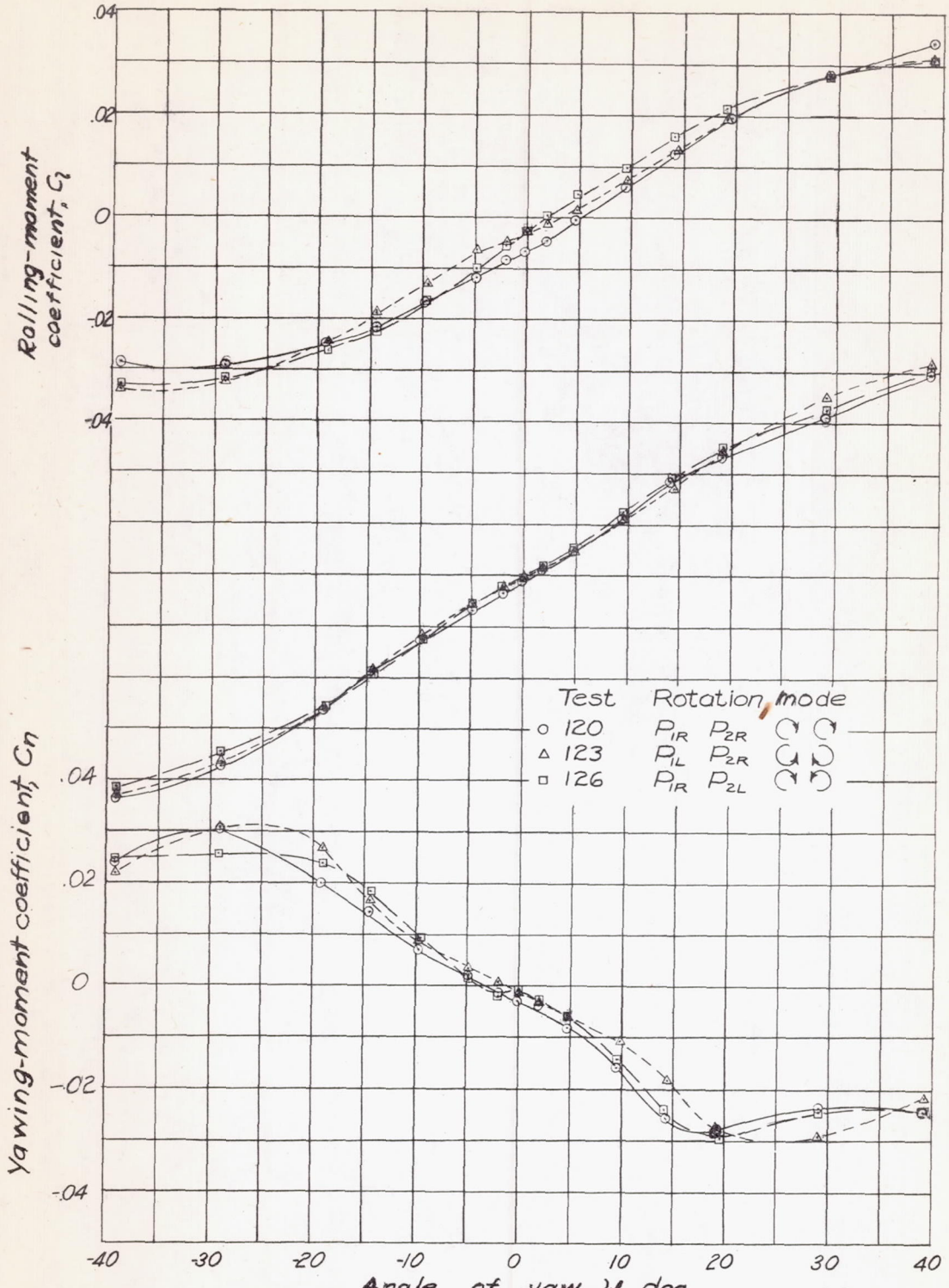

(b) Variation of C_n, C_l, and C_y with ψ.

Figure 15.-Concluded.

(measure with 5/16")

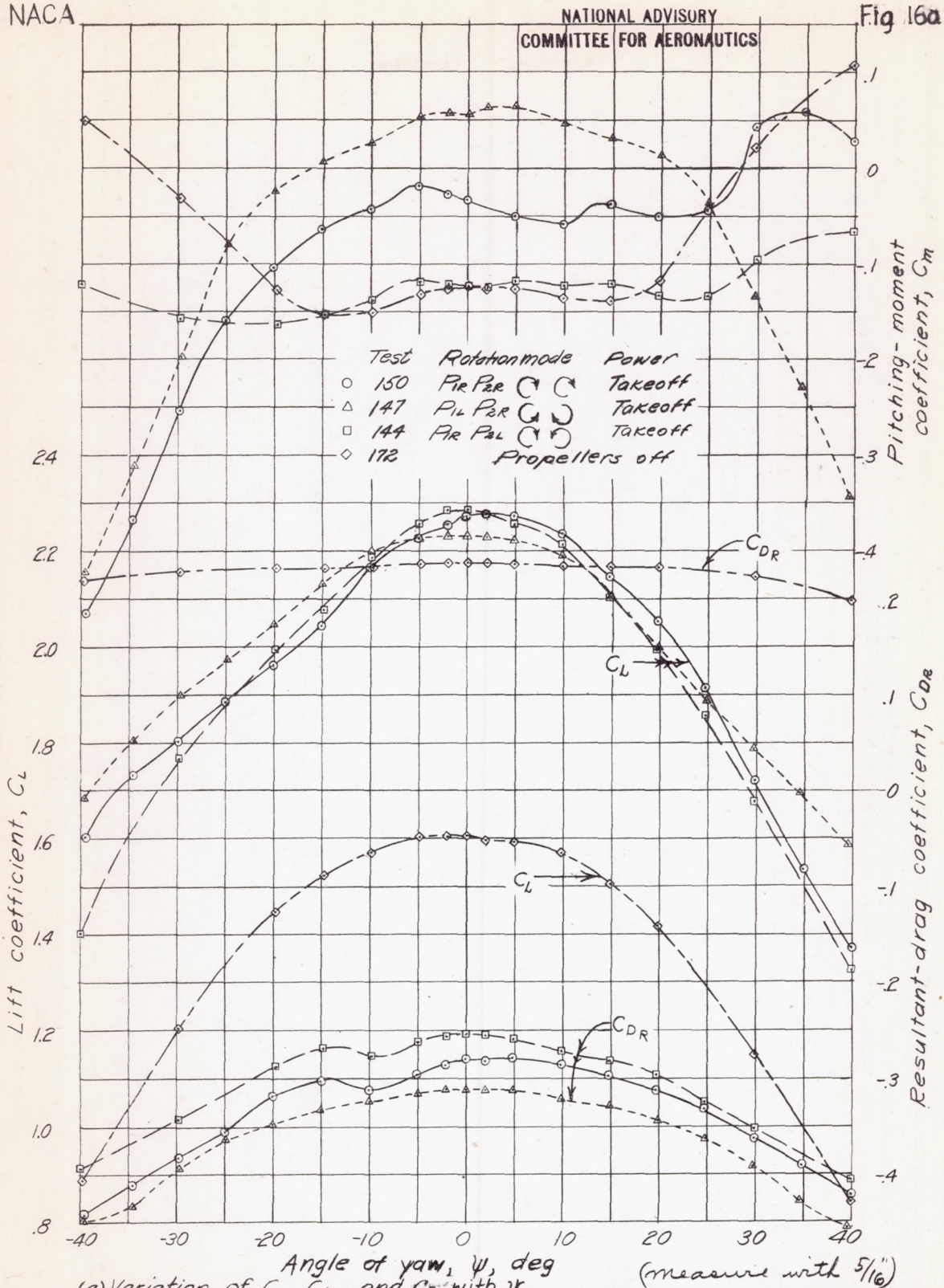

(a) Variation of C_L, C_m, and C_{D_R} with ψ.

Figure 16.- Effect of power and propeller rotation on the aerodynamic characteristics in yaw of the 1/10-scale complete model of the North American XB-28 airplane. Landing condition; landing gear down; cowl flaps closed; β, 27.1°; δ_a, δ_r, δ_e, 0°; δ_{f_1}, 45°; δ_{f_2}, 40°; q, 4.09 pounds per square foot.

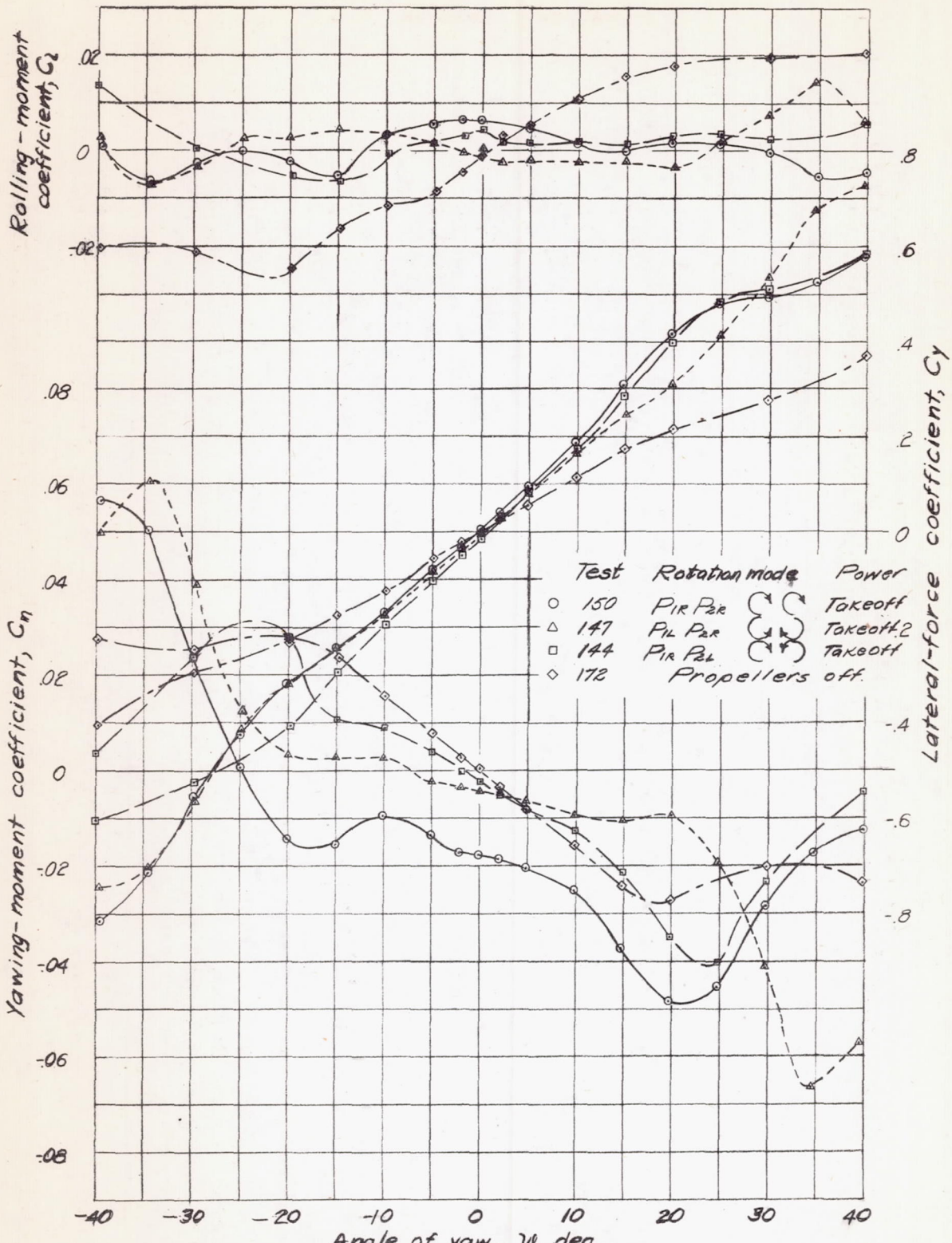

(b) Variation of C_n, C_l, and C_y with ψ.

Figure 16.- Concluded.

(measure with 5/16")

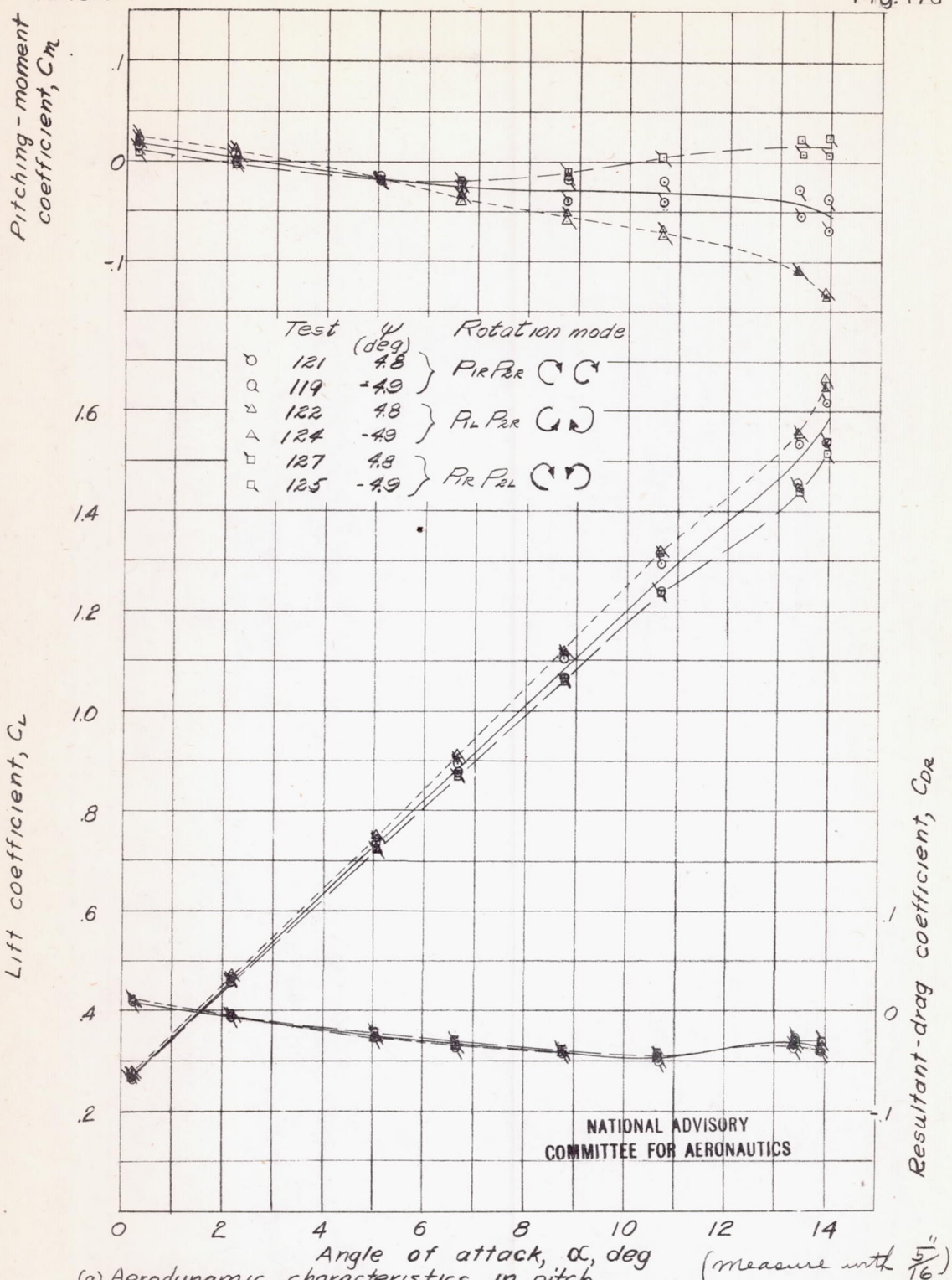

(a) Aerodynamic characteristics in pitch.

Figure 17.- Effect of propeller rotation on the aerodynamic characteristics of the 1/10-scale complete model of the North American XB-28 airplane. High-speed condition; landing gear up; cowl flaps closed; rated power; β, 40.5°; δ_a, δ_e, δ_r, δ_f, 0°; q, 16.37 pounds per square foot.

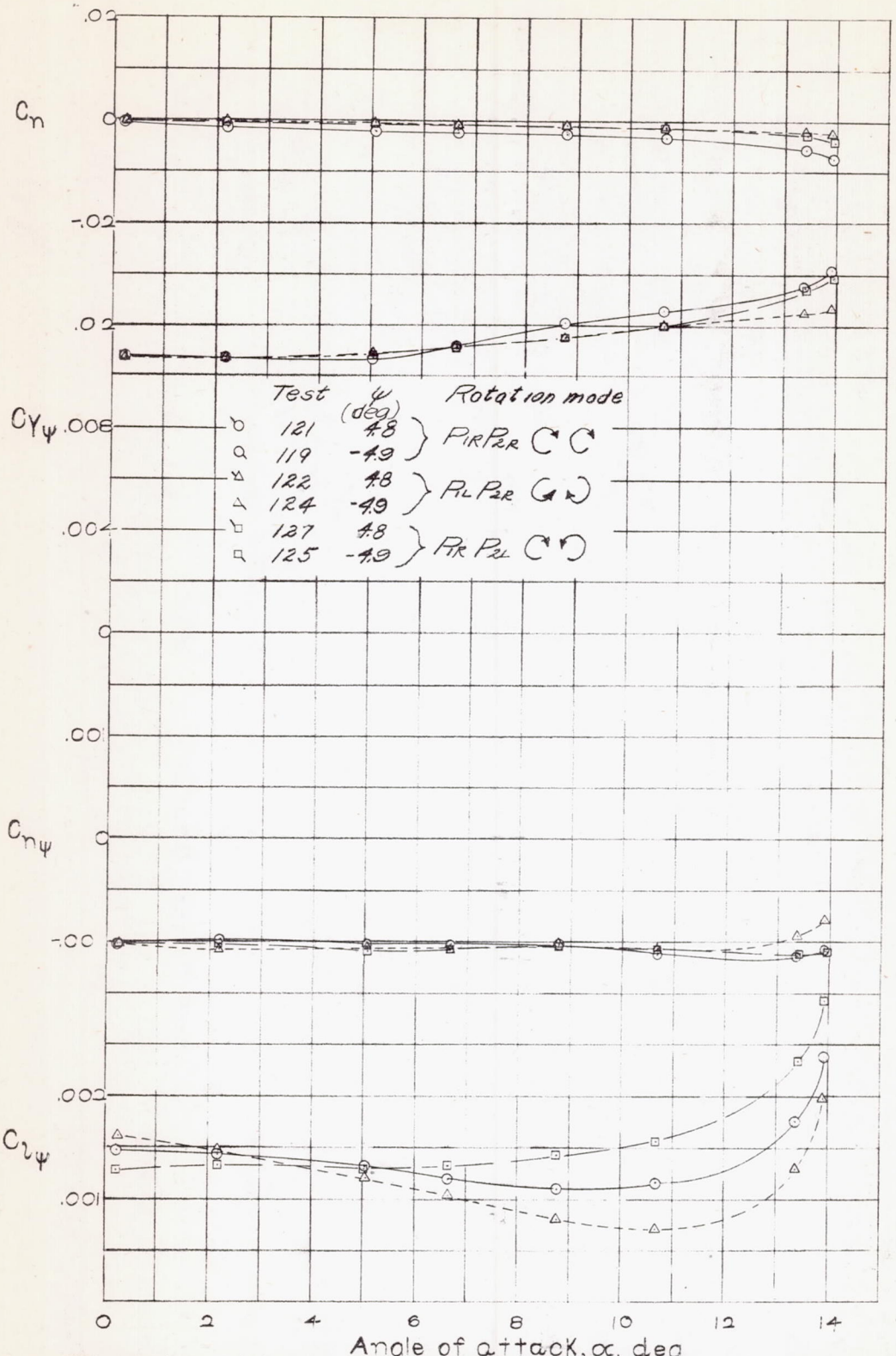

(b) Static-stability derivatives in yaw.

Figure 17.- Concluded.

(Measure with 5/16")

L-295

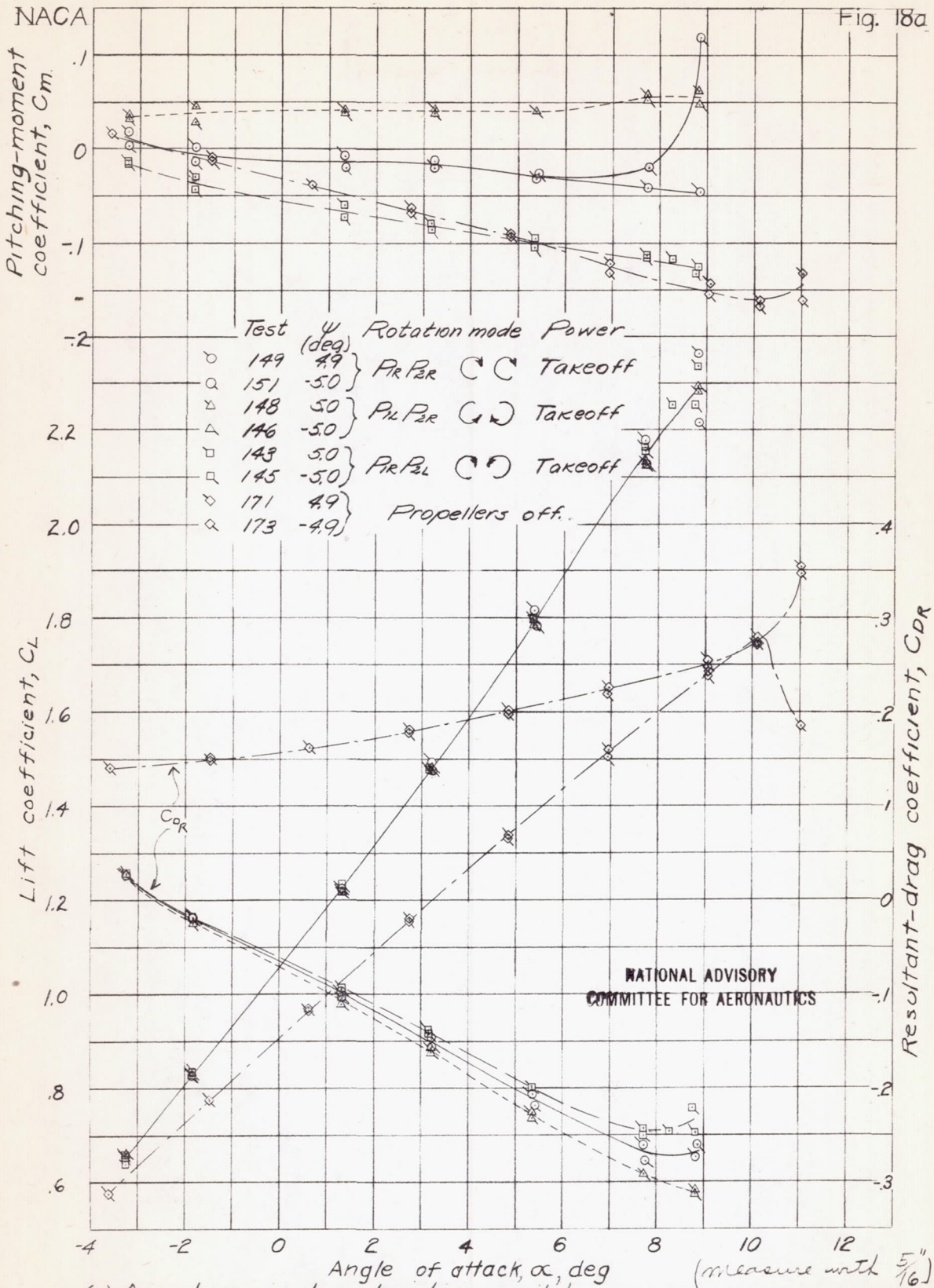

(a) Aerodynamic characteristics in pitch.

Figure 18.- Effect of power and propeller rotation on the aerodynamic characteristics of the 1/10-scale complete model of the North American XB-28 airplane. Landing condition; landing gear down; cowl flaps closed; ; β, 27.1°; δ_a, δ_e, δ_r, 0°; δ_{f_1}, 45°; δ_{f_2}, 40°; q, 4.09 pounds per square foot.

NACA

Fig. 18b

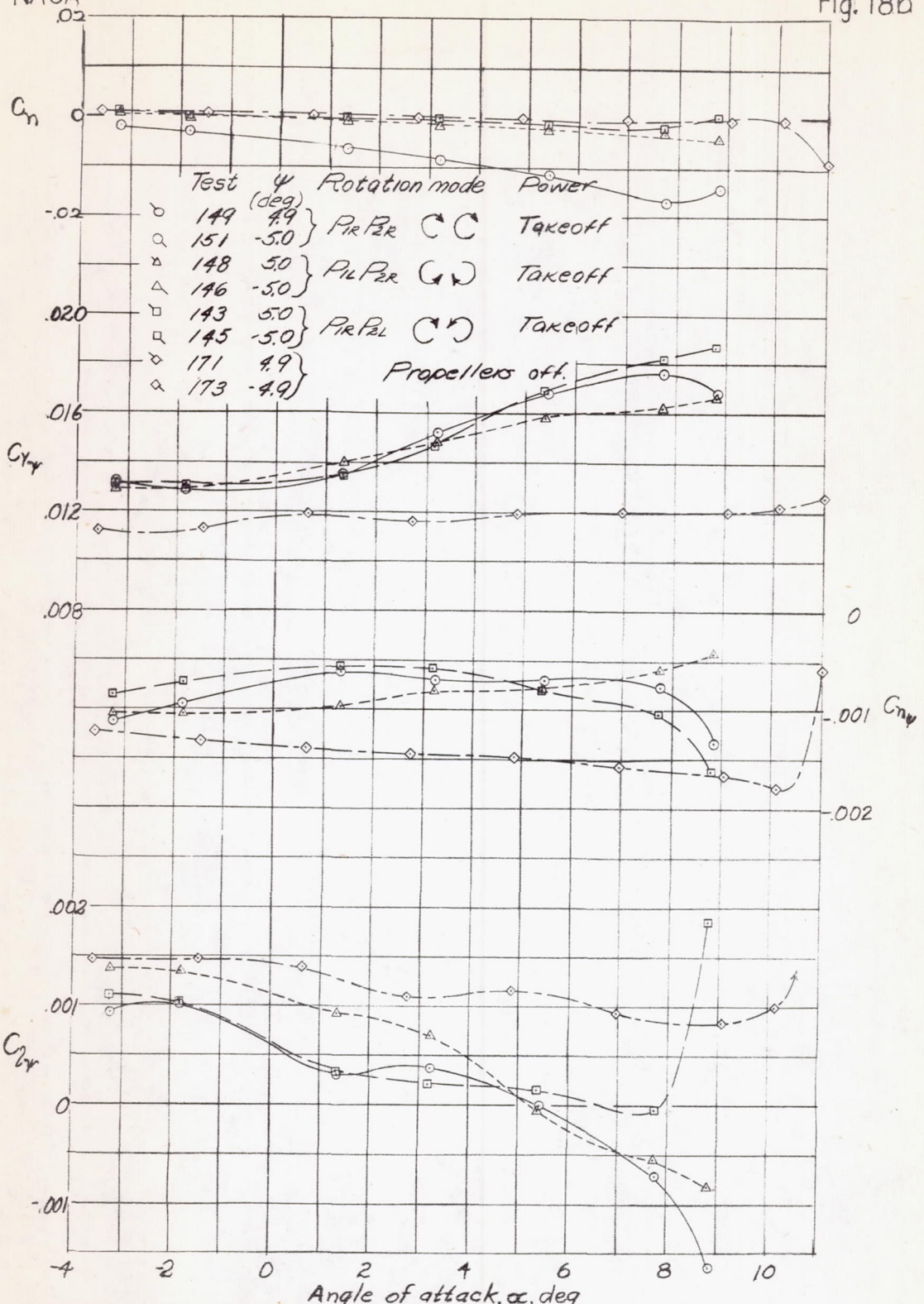

(b) Static-stability derivatives in yaw.

Figure 18.- Concluded.

(measure with 5/16")

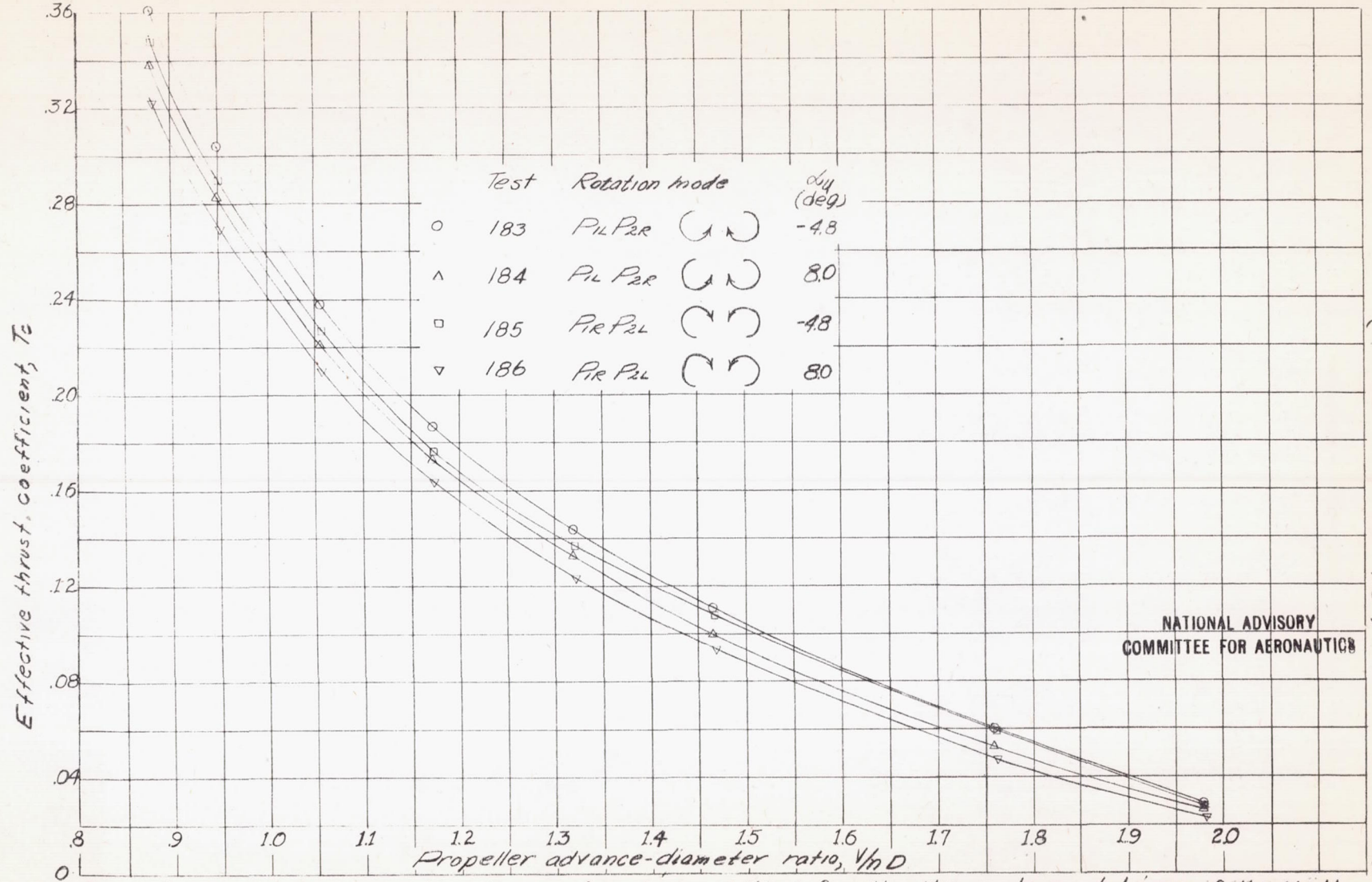

NACA (measure with 5/16")

Fig. 19

Figure 19.- Effective thrust coefficient as a function of V/nD for the 1/10-scale model wing of the North American XB 28 airplane. High-speed condition; landing gear up; β, 90.5°; δ_f, 0°; q, 16.37 pounds per square foot.

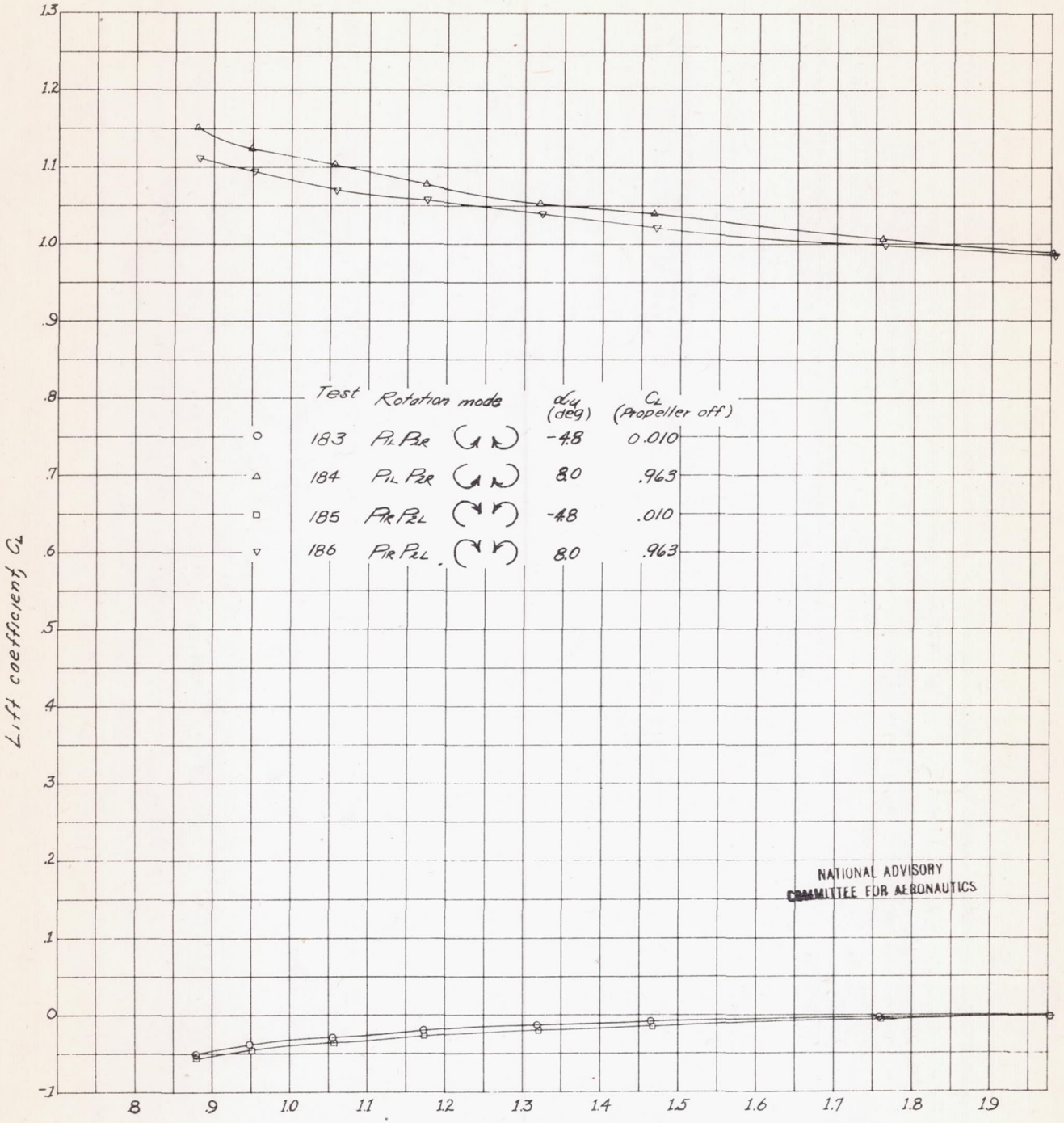

Figure 20.- Lift coefficients at given tunnel angle of attack and propeller rotation made as functions of V/nD for the 1/10-scale model wing of North American XB-28 airplane. High-speed condition, landing gear up; β, 40.5°; δ_f, 0°; q, 16.37 pounds per square foot.

NACA

Fig. 21a

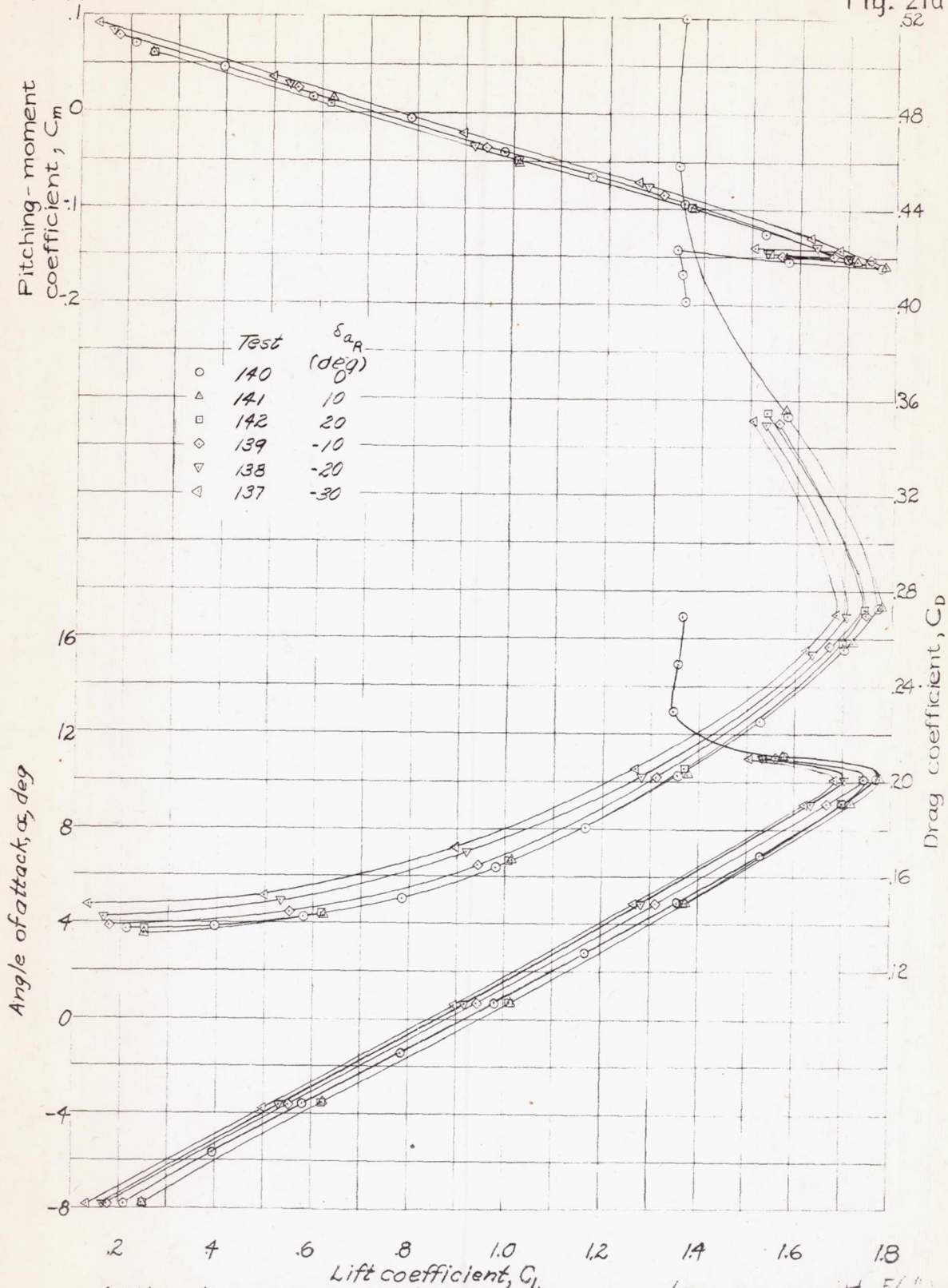

(a) Variation of α, C_m, and C_D with C_L. (measure with 5/16")

FIGURE 21. - Effect of right aileron deflection on the power-off aerodynamic characteristics in pitch of the 1/10-scale model of the North American XB-28 airplane. Landing condition; landing gear down; δ_e, δ_r, 0°; δ_{f_1}, 45°; δ_{f_2}, 40°; q, 4.09 pounds per square foot.

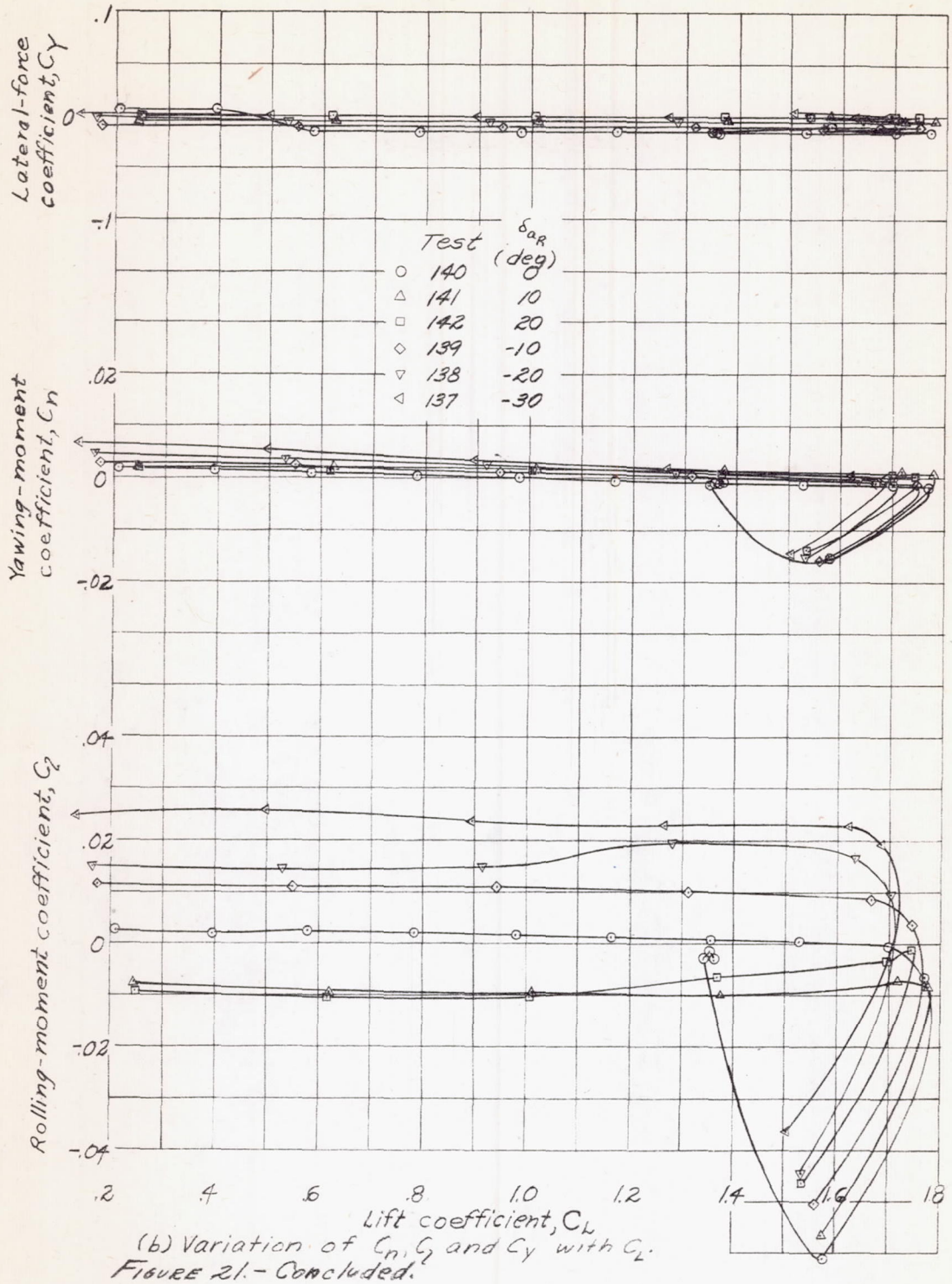

(b) Variation of C_n, C_l and C_Y with C_L.

FIGURE 21.- Concluded.